

Performance Analysis Framework for Transmit Antenna Selection Strategies of Cooperative MIMO AF Relay Networks

Gayan Amarasuriya, *Student Member, IEEE*, Chintla Tellambura, *Fellow, IEEE*, and Masoud Ardakani, *Senior Member, IEEE*

Abstract—The performance of three transmit antenna selection (TAS) strategies for dual-hop multiple-input–multiple-output (MIMO) ideal channel-assisted amplify-and-forward (AF) relay networks is analyzed. All channel fades are assumed to be Nakagami- m (integer m) fading. The source, relay, and destination are MIMO terminals. The optimal TAS and two suboptimal TAS strategies are considered. Since direct analysis of the end-to-end signal-to-noise ratio (e2e SNR) of the optimal TAS is intractable, a lower bound of the e2e SNR is derived. Its cumulative distribution function and the moment generating function (mgf) are derived and used to obtain the upper bounds of the outage probability and the average symbol error rate (SER). For the two suboptimal TAS strategies, we derive the exact mgfs of the e2e SNR and obtain accurate and efficient closed-form approximations for the outage probability and the average SER. The asymptotic outage probability and the average SER, which are exact in high SNR, are also derived, and they provide valuable insights into the system design parameters, such as diversity order and array gain. The exact outage probability, average SER, and their high SNR approximations are also derived for the optimal TAS when the direct path is ignored. The impact of outdated channel state information (CSI) on the performance of TAS is also studied. Specifically, the amount of performance degradation due to feedback delays is studied by deriving the asymptotic outage probability and the average SER and thereby quantifying the reduction of diversity order and array gain. Numerical and Monte Carlo simulation results are provided to analyze the system performance and verify the accuracy of our analysis.

Index Terms—Amplify-and-forward (AF) relaying, cooperative multiple-input–multiple-output (MIMO) relay networks, transmit antenna selection (TAS).

I. INTRODUCTION

COOPERATIVE relay networks are currently being investigated for emerging wireless system standards, such as IEEE 802.16m and Third-Generation Partnership Project Long Term Evolution-Advanced [1], [2]. The performance of

Manuscript received September 14, 2010; revised January 2, 2011 and March 15, 2011; accepted April 16, 2011. Date of publication May 23, 2011; date of current version September 19, 2011. This work was supported in part by Alberta Innovates Technology Future graduate student scholarship program. This paper was presented in part at IEEE Global Communications Conference, Miami, FL, December 2010. The review of this paper was coordinated by Prof. H.-F. Lu.

The authors are with the Department of Electrical and Computer Engineering, University of Alberta, Edmonton, AB T6G 2V4, Canada (e-mail: amarasur@ece.ualberta.ca; chintla@ece.ualberta.ca; ardakani@ece.ualberta.ca).

Color versions of one or more of the figures in this paper are available online at <http://ieeexplore.ieee.org>.

Digital Object Identifier 10.1109/TVT.2011.2157371

such relay networks can be improved by integrating multiple-input–multiple-output (MIMO) technology [3], [4] and transmit antenna selection (TAS) [5]–[10]. Although TAS is a suboptimal beamforming technique, it substantially reduces the complexity and power requirements of the transmitter. Further, it is more robust against channel estimation errors and time variations of the channels than other beamforming techniques, for example, transmit diversity [11], [12]. The current TAS strategies for general MIMO relay networks [5], [6] lack a suitable performance analysis framework.

Prior Related Research: The optimal TAS strategy (TAS_{opt}) for dual-hop MIMO amplify-and-forward (AF) cooperative relay networks involves maximizing the end-to-end (e2e) signal-to-noise ratio (SNR) by selecting the best transmit antenna at the source and relay by an exhaustive search [5]. Although TAS_{opt} achieves the full diversity order of the MIMO relay channel, its implementation complexity is relatively high due to the requirement of the channel state information (CSI) of all three channels (i.e., $S \rightarrow D$, $S \rightarrow R$, and $R \rightarrow D$) at the source. As a remedy, Cao *et al.* [6] propose two suboptimal yet low-complexity TAS strategies (referred to as TAS_{subopt_1} and TAS_{subopt_2}). The complexity reduction is achieved by maximizing the individual channel SNRs rather than the e2e SNR. More specifically, TAS_{subopt_1} maximizes the source-to-destination ($S \rightarrow D$) and relay-to-destination ($R \rightarrow D$) SNRs, whereas TAS_{subopt_2} maximizes the source-to-relay ($S \rightarrow R$) and $R \rightarrow D$ SNRs. In particular, TAS_{subopt_1} and TAS_{subopt_2} require only the CSI of either $S \rightarrow D$ or $S \rightarrow R$ channels only. This reduction of CSI feedback and, thereby, the implementation complexity is the main motivation behind the TAS_{subopt_1} and TAS_{subopt_2} strategies. The performance of these three TAS strategies has been evaluated by using Monte Carlo simulations only without analysis [5], [6]. Recently, in [13], we investigated the performance of these three TAS strategies for MIMO AF relay networks over Rayleigh fading.

Other studies of TAS for MIMO AF relaying [7]–[10], [14]–[18] differ from [5] and [6]. These studies either employ TAS for only one S or R , or they all ignore the $S \rightarrow D$ direct path. Thus, their TAS algorithms are completely different from those of TAS_{opt} , TAS_{subopt_1} , and TAS_{subopt_2} in [5] and [6]. In [7], the outage probability of multihop MIMO relaying with TAS is derived semianalytically. In [8], the relay is limited to a single antenna, and the source and the destination employ TAS and maximal ratio combining (MRC), respectively. The outage and the average symbol error rate (SER) are derived. In

[9], transmit/receive (Tx/Rx) antenna pair selection is proposed for dual-hop MIMO AF relay networks. Here, the e2e transmission takes place by selecting the best Tx/Rx antenna pair at both $S \rightarrow R$ and $R \rightarrow D$ MIMO channels. Reference [10] extends [9] by deriving the asymptotic outage probability and average SER. In addition, [19] extends the analysis of [9] for Nakagami- m fading. In [14], the diversity order of a suboptimal TAS for MIMO relay networks is derived. In [16]–[18], the performance of TAS for dual-hop AF relay networks is studied by ignoring the direct path between S and D . Further, in [15], three TAS strategies, which are optimal in terms of the outage probability, are developed for MIMO decode-and-forward relaying.

Motivation and Our Contribution: Although [5] derives the diversity order of TAS_{opt} , no closed-form performance metrics are derived. Moreover, [5] resorts to Monte Carlo simulations for the comparison of the average bit error rate (BER) of binary phase-shift keying (BPSK) with that of several MIMO AF beamforming strategies. Furthermore, [6] also utilizes the Monte Carlo simulation framework for the performance of the TAS_{subopt_1} and TAS_{subopt_2} strategies. In summary, an analytical framework for the TAS strategies of [5] and [6] for MIMO AF relay networks is not available. Our main contribution is thus to fill this gap.

In this paper, the performance of the three aforementioned TAS strategies is analyzed. All channel fades are assumed to be Nakagami- m (integer m) fading. Since direct analysis of the e2e SNR of the optimal TAS is intractable, a lower bound of the e2e SNR is derived. Its cumulative distribution function (cdf) and the moment generating function (mgf) are derived, and the upper bounds for the outage probability and the average SER of TAS_{opt} are obtained. For TAS_{subopt_1} and TAS_{subopt_2} , which, however, are amenable to exact analysis, we derive the exact mgfs of the e2e SNRs and obtain the outage probability and average SER approximations.¹ The asymptotic performance measures, which are exact in high SNR, are also derived and provide valuable insights about the system design parameters, such as the diversity order and the array gain. The closed-form exact outage probability, average SER, and their high SNR approximations are also derived for the optimal TAS when the direct path is ignored. Finally, the impact of outdated CSI due to feedback delays on the performance of TAS_{opt} is studied. Specifically, the amount of performance degradation is quantified by deriving the exact asymptotic outage probability and average SER and thereby deriving the reduction in diversity order and array gain. Numerical and Monte Carlo simulation results are also provided to analyze the system performance and to verify the accuracy of our analytical framework.

The rest of this paper is organized as follows: Section II presents the system and the channel model. Section III summarizes the three TAS strategies. In Section IV, the performance analysis is presented. Section V contains the numerical and simulation results. Section VI concludes this paper. The proofs are given in the Appendix.

¹The main motivation behind our analysis of TAS_{subopt_1} and TAS_{subopt_2} is that they require significantly less CSI feedback at S than the TAS_{opt} , and thus, suboptimal TAS strategies can readily be employed in practical system designing.

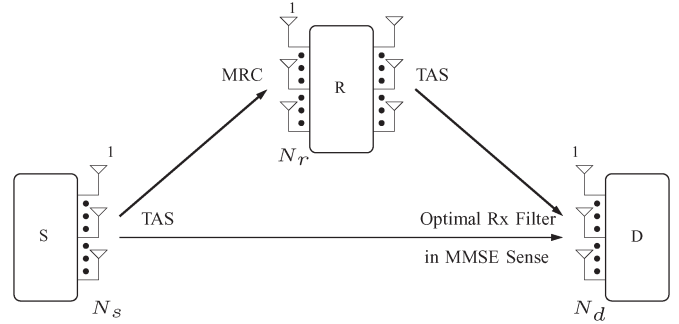


Fig. 1. Selection of the transmit antenna at the source (S) and relay (R) for MIMO AF relay networks: System model.

Notations: $\mathcal{K}_\nu(z)$ is the modified Bessel function of the second kind of order ν [20, eq. (8.407.1)]. ${}_2\mathcal{F}(\alpha, \phi; \gamma; z)$ is the Gauss hypergeometric function [20, eq. (9.14.1)]. $\mathbb{I}_\nu(z)$ is the modified Bessel function of the first kind of order ν [20, eq. (8.406.1)]. $\mathbb{M}_{\nu, \mu}(z)$ is the Whittaker-M function [20, eq. (9.220.2)]. $\mathcal{Q}(z)$ denotes the Gaussian Q -function [21, eq. (26.2.3)]. $\Re\{z\}$ is the real part of z . $\|\mathbf{Z}\|_F$ is the Frobenius norm of \mathbf{Z} . A circular symmetric complex Gaussian distributed random variable with mean μ and variance σ^2 is defined by $z \sim \mathcal{CN}(\mu, \sigma^2)$. $\gamma \sim \mathcal{G}(\alpha, \beta)$ is Gamma distributed with the probability density function (pdf) $f_\gamma(x) = (x^{\alpha-1} e^{-x/\beta} / \Gamma(\alpha)\beta^\alpha)$, $x \geq 0$, where α and β are the shape and scale parameters.

II. SYSTEM MODEL

We consider a dual-hop cooperative relay network with MIMO-enabled S , R , and D having N_s , N_r , and N_d antennas, respectively (see Fig. 1). All the terminals operate in half-duplex mode, and cooperation takes place in two time slots [22]. Perfect CSI is assumed at R and D , and the feedback channels are assumed to be perfect unless otherwise stated. The channel matrix from terminal X to terminal Y , where $X \in \{S, R\}$, $Y \in \{R, D\}$, and $X \neq Y$, is denoted by \mathbf{H}_{XY} . The elements of \mathbf{H}_{XY} are denoted by $h_{XY}^{i,j}$. The channel gains are assumed to be independent and identical Nakagami- m fading (with integer m). The channel vector from the j th transmit antenna at X to Y is denoted by $\mathbf{h}_{XY}^{(j)}$. Moreover, the additive noise at the nodes is modeled as complex zero-mean white Gaussian noise.

In the first time slot, S broadcasts to R and D by TAS, and R employs MRC reception. Here, we consider an ideal channel-assisted AF (CA-AF) relay² with a gain $G = 1/\|\mathbf{h}_{SR}^{(i)}\|_F^2$ [7], [23], [24] for the sake of mathematical tractability of the mgf of the e2e SNR. In the second time slot, relay R amplifies and forward the received signal to D again by TAS. Then, D combines the two signals received in the two time slots by applying the optimal receiver filter in the minimum mean-square error sense [5], [8]. Under this system model, the postprocessing e2e

²The ideal CA-AF relays invert the source-to-relay channel gain, regardless of its fading state. The performance metrics obtained by using ideal CA-AF relays serves as extremely tight (in low-to-high SNR regime) and asymptotically exact lower bounds to that of practical CA-AF relays [7], [23], [24], in which the relay gain is given by $G = \sqrt{1/\|\mathbf{h}_{SR}^{(i)}\|_F^4 + \sigma^2}$, where σ^2 is the noise variance. Specifically, the performance metrics derived by using ideal CA-AF relays serve as useful benchmarks for practical CA-AF relay network designing [23].

SNR at D when S and R use the i th and k th transmit antennas is given by [5]

$$\gamma_{eq}^{(i,k)} = \gamma_{SD}^{(i)} + \frac{\gamma_{SR}^{(i)} \gamma_{RD}^{(k)}}{\gamma_{SR}^{(i)} + \gamma_{RD}^{(k)}} \quad (1)$$

where $\gamma_{SD}^{(i)} = \bar{\gamma}_{SD} \|\mathbf{h}_{SD}^{(i)}\|_F^2$, $\gamma_{SR}^{(i)} = \bar{\gamma}_{SR} \|\mathbf{h}_{SR}^{(i)}\|_F^2$, and $\gamma_{RD}^{(k)} = \bar{\gamma}_{RD} \|\mathbf{h}_{RD}^{(k)}\|_F^2$ are the equivalent instantaneous SNRs, and $\bar{\gamma}_{SD}$, $\bar{\gamma}_{SR}$, and $\bar{\gamma}_{RD}$ are the average SNRs of the $S \rightarrow D$, $S \rightarrow R$, and $R \rightarrow D$ channels, respectively. Here, $\gamma_{SD}^{(i)}$, $\gamma_{SR}^{(i)}$, and $\gamma_{RD}^{(k)}$ are independent Gamma distributed random variables; $\gamma_{SD}^{(i)} \sim \mathcal{G}(M_0, \beta_0)$, $\gamma_{SR}^{(i)} \sim \mathcal{G}(M_1, \beta_1)$, and $\gamma_{RD}^{(k)} \sim \mathcal{G}(M_2, \beta_2)$, where $M_0 = m_0 N_d$, $M_1 = m_1 N_r$, $M_2 = m_2 N_d$, $\beta_0 = (\bar{\gamma}_{SD}/m_0)$, $\beta_1 = (\bar{\gamma}_{SR}/m_1)$, and $\beta_2 = (\bar{\gamma}_{RD}/m_2)$. Further, m_0 , m_1 , and m_2 are the integer severities of the fading parameters of the Nakagami fading in the $S \rightarrow D$, $S \rightarrow R$, and $R \rightarrow D$ channels.

III. TRANSMIT ANTENNA SELECTION STRATEGIES

For the sake of completeness, this section summarizes the optimal TAS and two suboptimal TAS strategies for the AF MIMO relaying proposed in [5] and [6], respectively.

A. Optimal TAS for AF MIMO Relaying (TAS_{opt})

The e2e SNR $\gamma_{eq}^{(i,k)}$ for AF MIMO relaying, (1) can be maximized by selecting the best transmit antenna at S and R as follows [5]:

$$(I, K) = \arg \max_{1 \leq i \leq N_s, 1 \leq k \leq N_r} \left(\gamma_{eq}^{(i,k)} \right) \quad (2)$$

where I and K are the optimal antenna indexes at S and R , and $\arg \max_{\theta} f(\theta)$ is the value of θ for which $f(\theta)$ is the largest.

B. Suboptimal TAS for AF MIMO Relaying

The search complexity and the amount of CSI feedback of TAS_{opt} is high since the transmit antenna at S [i.e., antenna index I in (2)] should be searched to maximize $\gamma_{eq}^{(i,k)}$ by considering both $S \rightarrow R$ and $S \rightarrow D$ channel SNRs. In [6], two suboptimal TAS strategies are proposed, providing a better tradeoff between the implementation complexity and the performance, as follows:

- 1) TAS_{subopt_1} : TAS is used at S and R separately to maximize the SNR of the $S \rightarrow D$ and $R \rightarrow D$ channels, respectively. The antenna indices are obtained as

$$I = \arg \max_{1 \leq i \leq N_s} \left(\gamma_{SD}^{(i)} \right) \quad \text{and} \quad K = \arg \max_{1 \leq k \leq N_r} \left(\gamma_{RD}^{(k)} \right). \quad (3)$$

- 2) TAS_{subopt_2} : TAS is used at S and R separately to maximize the SNR of the $S \rightarrow R$ and $R \rightarrow D$ channels, respectively. The antenna indices are selected as

$$I = \arg \max_{1 \leq i \leq N_s} \left(\gamma_{SR}^{(i)} \right) \quad \text{and} \quad K = \arg \max_{1 \leq k \leq N_r} \left(\gamma_{RD}^{(k)} \right). \quad (4)$$

Remark III.1: In practice, the direct path between S and D may be unavailable entirely due to heavy shadowing and path loss. In this scenario, the optimal TAS strategy selects

the transmit antennas at S and R separately to maximize the SNR of the $S \rightarrow R$ and $R \rightarrow D$ channels, respectively, without considering the $S \rightarrow D$ channel. Under this scenario, the TAS strategy is given by [13]

$$I = \arg \max_{1 \leq i \leq N_s} \left(\gamma_{SR}^{(i)} \right) \quad \text{and} \quad K = \arg \max_{1 \leq k \leq N_r} \left(\gamma_{RD}^{(k)} \right). \quad (5)$$

IV. PERFORMANCE ANALYSIS

This section presents our performance analyses of the TAS strategies given in (2)–(4). Since the exact analysis of TAS_{opt} appears to be mathematically intractable, a lower bound of the e2e SNR of TAS_{opt} is used. The cdf and the mgf of this lower bound are derived in closed form and used to obtain the closed-form upper bounds for the outage probability and the average SER. The exact mgfs of the e2e SNRs of TAS_{subopt_1} and TAS_{subopt_2} are derived as well. Accurate closed-form approximations of the outage probability and average SER are presented for each suboptimal TAS strategy by using efficient numerical techniques. Further, the corresponding asymptotic results are also derived.

A. Statistical Characterization of the e2e SNR

1) *cdf of the e2e SNR for TAS_{opt}* : Let γ_{eq}^{opt} denote the e2e SNR at D for TAS_{opt} . In (2), for fixed $\gamma_{SD}^{(i)}$ and $\gamma_{SR}^{(i)}$, $\gamma_{eq}^{(i,k)}$ is maximized when $\gamma_{RD}^{(k)}$ is maximized, i.e., the TAS at R is independent of the TAS at S . Thus, in TAS_{opt} , the antenna indexes I and K can be selected as

$$K = \arg \max_{1 \leq k \leq N_r} \left(\gamma_{RD}^{(k)} \right) \quad \text{and} \quad I = \arg \max_{1 \leq i \leq N_s} \left(\gamma_{eq}^{(i,K)} \right). \quad (6)$$

The upper bound³ of the cdf of γ_{eq}^{opt} in (32) can then be derived as (see Appendix A for the proof)

$$F_{\gamma_{eq,lb}^{opt}}(x) = \left[1 - \sum_{a,b,p,q,l} \mathcal{A}_1 x^{M_2+b+q} e^{-x\kappa} \mathcal{K}_{l-b+1}(x\lambda) \right] \times \left[\sum_{u=0}^{N_s} \sum_{v=0}^{u(M_2-1)} \mathcal{B}_1 x^v e^{-\frac{ux}{\beta_0}} \right] \quad (7a)$$

where \mathcal{A}_1 , \mathcal{B}_1 , κ , and λ are defined as

$$\mathcal{A}_1 = \frac{2N_r \binom{N_s}{a} \binom{N_r-1}{p} \binom{M_1+b+q-1}{l} (-1)^{a+p+1} \phi_{b,a,M_1} \phi_{q,p,M_2}}{\Gamma(M_2) a^{\frac{b-l-1}{2}} (p+1)^{\frac{l-b+1}{2}} \beta_1^{\frac{l+b+1}{2}} \beta_2^{\frac{2M_2+2q-l+b-1}{2}}} \quad (7b)$$

$$\mathcal{B}_1 = (-1)^u \binom{N_s}{u} \frac{\phi_{v,u,M_0}}{\beta_0}, \quad \kappa = \frac{a}{\beta_1} + \frac{p+1}{\beta_2} \quad \text{and} \quad (7c)$$

$$\lambda = 2\sqrt{\frac{a(p+1)}{\beta_1\beta_2}}. \quad (7d)$$

³Alternatively, (7a) can be seen as the cdf of the lower bound of the e2e SNR in (32). Specifically, this SNR lower bound is given by $\gamma_{eq,lb}^{opt} = \max_{1 \leq i \leq N_s} \{ \gamma_{SD}^{(i)}, \gamma_{SR}^{(i,K)} \}$. In general, the SNR lower bound, which underestimates the exact SNR, results in the outage probability upper bound.

Further, $\sum_{a,b,p,q,l} = \sum_{a=1}^{N_s} \sum_{b=0}^{a(M_1-1)} \sum_{p=0}^{N_r-1} \sum_{q=0}^{p(M_2-1)}$ and $\phi_{k,N,L}$ is the coefficient of the expansion of $[\sum_{u=0}^{L-1} (1/u!)(x/\bar{\gamma})^u]^N = \sum_{k=0}^{N(L-1)} \phi_{k,N,L}(x/\bar{\gamma})^k$ and given by [25, eq. (44)]

$$\phi_{k,N,L} = \sum_{i=k-L+1}^k \frac{\phi_{i,N-1,L}}{(k-i)!} I_{[0,(N-1)(L-1)]}(i). \quad (8)$$

2) *mgf of the e2e SNR for TAS_{opt}*: The mgf of $\gamma_{\text{eq,lb}}^{\text{opt}}$ can be derived by substituting (7a) into $\mathcal{M}_{\gamma_{\text{eq,lb}}^{\text{opt}}}(s) = \mathcal{E}_{\gamma_{\text{eq,lb}}^{\text{opt}}} \{e^{-s\gamma}\} = \int_0^\infty sF_{\gamma_{\text{eq,lb}}^{\text{opt}}}(\gamma)e^{-s\gamma}d\gamma$ and by using [20, eq. (6.621.3)] as follows:

$$\begin{aligned} \mathcal{M}_{\gamma_{\text{eq,lb}}^{\text{opt}}}(s) &= \sum_{u=0}^{N_s} \sum_{v=0}^{u(M_0-1)} \mathcal{B}_1 \beta_0^2 \Gamma(v+1) \frac{s}{(u+s\beta_0)^{v+1}} \\ &- \sum_{a,b,p,q,l} \sum_{u=0}^{N_s} \sum_{v=0}^{m(M_0-1)} \frac{\mathcal{A}_1 \sqrt{\pi} (-1)^u (2\lambda)^\zeta \Gamma(\eta+\zeta) \Gamma(\eta-\zeta)}{\beta_0^v \Gamma(\eta+\frac{1}{2})} \\ &\times \frac{s {}_2\mathcal{F}_1\left(\eta+\zeta, \zeta+\frac{1}{2}; \eta+\frac{1}{2}; \frac{s+\kappa-\lambda}{s+\kappa+\lambda}\right)}{(s+\kappa+\lambda)^{\eta+\zeta}} \end{aligned} \quad (9)$$

where $\sum_{a,b,p,q,l}$ is defined in (7a). Further, η , ζ , κ , and λ depend on the summation variables and are defined as $\eta = M_2 + b + q + v + 1$, $\zeta = l - b + 1$, $\kappa = (a/\beta_1) + (p + 1/\beta_2)$, and $\lambda = 2\sqrt{a(p+1)/\beta_1\beta_2}$, respectively.

The pdf of $\gamma_{\text{eq,lb}}^{\text{opt}}$ can readily be derived by differentiating the cdf of $\gamma_{\text{eq,lb}}^{\text{opt}}$ with respect to x by using [20, eq. (8.486.12)]. However, the pdf result is omitted for the sake of brevity.

3) *mgf of the e2e SNR for TAS_{subopt1}*: Let $\gamma_{\text{eq}}^{\text{subopt1}}$ denote the e2e SNR at D for TAS_{subopt1}. Define $\mathcal{M}_{\gamma_{\text{SRD}}^{\text{subopt1}}}(s)$ as the mgf of the SNR of the relayed path and given by

$$\begin{aligned} \mathcal{M}_{\gamma_{\text{SRD}}^{\text{subopt1}}}(s) &= 1 - \sum_{a=1}^{N_r} \sum_{b=0}^{a(M_2-1)} \sum_{c=0}^{b+M_1-1} \frac{\mathcal{A}_2 \sqrt{\pi} (2\nu)^\zeta \Gamma(\eta+\zeta)}{\Gamma(\eta+\frac{1}{2})} \\ &\times \frac{\Gamma(\eta-\zeta) s {}_2\mathcal{F}_1\left(\eta+\zeta, \zeta+\frac{1}{2}; \eta+\frac{1}{2}; \frac{s+\mu-\nu}{s+\mu+\nu}\right)}{(s+\mu+\nu)^{\eta+\zeta}} \end{aligned} \quad (10a)$$

where \mathcal{A}_2 is given by

$$\mathcal{A}_2 = \frac{2(-1)^{a+1} \phi_{b,a,M_2} \binom{N_r}{a} \binom{b+M_1-1}{c} a^{\binom{\zeta}{2}}}{\Gamma(M_1) \beta_1^{\frac{2M_1+b-c-1}{2}} \beta_2^{\frac{c+b+1}{2}}}. \quad (10b)$$

Further, μ , η , ζ , and ν depend on the summation variables and are defined as $\mu = (1/\beta_1) + (a/\beta_2)$, $\eta = M_1 + b + 1$, $\zeta = c - b + 1$, and $\nu = 2\sqrt{a/\beta_1\beta_2}$. Similarly, the mgf of the direct path $\mathcal{M}_{\gamma_{\text{SD}}^{\text{subopt1}}}(s)$ is given by

$$\mathcal{M}_{\gamma_{\text{SD}}^{\text{subopt1}}}(s) = \sum_{p=0}^{N_s} \sum_{q=0}^{p(M_0-1)} \frac{\binom{N_s}{p} (-1)^p \phi_{q,p,M_0} \beta_0 \Gamma(q+1) s}{(s\beta_0+p)^{q+1}}. \quad (11)$$

See the Appendix B for the proof of (10a) and (11).

The mgf of $\gamma_{\text{eq}}^{\text{subopt1}}$ is then given by the product of (10a) and (11).

4) *mgf of the e2e SNR for TAS_{subopt2}*: Let $\gamma_{\text{eq}}^{\text{subopt2}}$ denote the e2e SNR at D for TAS_{subopt2}. Define $\mathcal{M}_{\gamma_{\text{SRD}}^{\text{subopt2}}}(s)$ as the mgfs of SNR of the relayed path and is given by

$$\begin{aligned} \mathcal{M}_{\gamma_{\text{SRD}}^{\text{subopt2}}}(s) &= 1 - \sum_{p,q,a,b,c} \frac{\mathcal{A}_3 \sqrt{\pi} (2\epsilon)^{c-q+1} \Gamma(\eta+\zeta) \Gamma(\eta-\zeta)}{\Gamma(\eta+\frac{1}{2})} \\ &\times \frac{s {}_2\mathcal{F}_1\left(\eta+\zeta, \zeta+\frac{1}{2}; \eta+\frac{1}{2}; \frac{s+\delta-\epsilon}{s+\delta+\epsilon}\right)}{(s+\delta+\epsilon)^{\eta+\zeta}} \end{aligned} \quad (12a)$$

where \mathcal{A}_3 is given by

$$\begin{aligned} \mathcal{A}_3 &= \frac{2(-1)^{p+q+1} N_s p^{\frac{\zeta}{2}} \binom{N_r}{p} \binom{N_s-1}{a} \binom{M_1+q+b-1}{c}}{\Gamma(M_1) (a+1)^{\frac{\zeta}{2}}} \\ &\times \frac{\phi_{q,p,M_2} \phi_{b,a,M_1}}{\beta_1^{\frac{2M_1+q+2b-c-1}{2}} \beta_2^{\frac{c+q+1}{2}}}. \end{aligned} \quad (12b)$$

In (12a), $\sum_{p,q,a,b,c} = \sum_{p=1}^{N_r} \sum_{q=0}^{p(M_2-1)} \sum_{a=0}^{N_s-1} \sum_{b=0}^{a(M_1-1)}$ $\sum_{c=0}^{M_1+q+b-1}$. The parameters δ , η , ζ , and ϵ depend on the summation variables and are defined as $\delta = (a + 1/\beta_1) + (p/\beta_2)$, $\eta = M_1 + b + q + 1$, $\zeta = c - q + 1$ and $\epsilon = 2\sqrt{p(a+1)/\beta_1\beta_2}$, respectively. The mgf of the SNR of the direct path $\mathcal{M}_{\gamma_{\text{SD}}^{\text{subopt2}}}(s)$ is given by

$$\mathcal{M}_{\gamma_{\text{SD}}^{\text{subopt2}}}(s) = (1 + \beta_0 s)^{M_0}. \quad (13)$$

See the Appendix D for the proof of (12a) and (13).

The mgf of the e2e SNR of TAS_{subopt2} is then given by the product of (12a) and (13).

B. Outage Probability

The SNR outage probability⁴ P_{out} is the probability that the instantaneous e2e SNR γ_{eq} falls below a threshold γ_{th} ; $P_{\text{out}} = \Pr(\gamma_{\text{eq}} \leq \gamma_{\text{th}}) = F_{\gamma_{\text{eq}}}(\gamma_{\text{th}})$, where $F_{\gamma_{\text{eq}}}(\gamma_{\text{th}})$ denotes the cdf of γ_{eq} evaluated at γ_{th} . An upper bound of P_{out} for TAS_{opt} can readily be obtained by using (7a). Further, P_{out} of TAS_{subopt1} and TAS_{subopt2} can accurately be computed by using [26], [27]

$$\begin{aligned} P_{\text{out}}^{\text{suboptj}} \Big|_{j=1}^2 &= F_{\gamma_{\text{eq}}^{\text{suboptj}}}(\gamma_{\text{th}}) = \frac{1}{5\gamma_{\text{th}}} \Psi \left(\frac{2N_p}{5\gamma_{\text{th}}} \right) e^{\frac{2N_p}{5}} \\ &+ \frac{2}{5\gamma_{\text{th}}} \sum_{k=1}^{N_p-1} \Re \left\{ e^{\gamma_{\text{th}} \Upsilon(\theta_k)} \Psi_j(\Upsilon(\theta_k)) (1 + i\Phi(\theta_k)) \right\} + R_{N_p} \end{aligned} \quad (14)$$

where $\Psi_j(s) \Big|_{j=1}^2 = \mathcal{M}_{\gamma_{\text{eq}}^{\text{suboptj}}}(s)/s$, $\theta_k = \pi k/N_p$, $\Upsilon(\theta) = (2N_p/5\gamma_{\text{th}})\theta(\cot\theta + i)$, $\Phi(\theta) = \theta + (\theta \cot\theta - 1) \cot\theta$, $i = \sqrt{-1}$, and R_{N_p} is the remainder term, which is negligible for a small number of terms (N_p), such as 20 (see Section V).

⁴The information capacity outage probability can be defined as the probability that the instantaneous mutual information \mathcal{I} falls below the target rate \mathcal{R}_{th} ; $\Pr(1/2 \log 1 + \gamma_{\text{eq}}) \leq \mathcal{R}_{\text{th}} = F_{\gamma_{\text{eq}}}(\gamma_{\text{th}})$, where $\gamma_{\text{th}} = 2^{2\mathcal{R}_{\text{th}}} - 1$.

C. Average SER

The conditional error probability (CEP) of the coherent BPSK and M -ary pulse amplitude modulation can be expressed as $P_e|\gamma = \alpha \mathcal{Q}(\sqrt{\varphi\gamma})$, where α and φ are modulation-dependent constants. The average SER can be derived by integrating CEP $P_e|\gamma$ over the pdf of the SNR γ_{eq} . Thus, an upper bound for the average SER of TAS_{opt} can be derived by substituting (7a) into $\bar{P}_e = (\alpha/2)\sqrt{\varphi/2\pi} \int_0^\infty x^{-1/2} e^{-\varphi x/2} F_{\gamma_{\text{eq}}}(x) dx$ and solving the resulting integral by using [20, eq. (6.621.3)] as follows:

$$\begin{aligned} \bar{P}_{e,ub}^{\text{TAS}_{\text{opt}}} &= \sum_{u=0}^{N_s} \sum_{v=0}^{u(M_2-1)} \frac{2^{v-1} \alpha \sqrt{\varphi} \beta_0^{\frac{3}{2}} \Gamma(v + \frac{1}{2})}{\sqrt{\pi} (2u + \varphi \beta_0)^{v + \frac{1}{2}}} \\ &\quad - \sum_{a,b,p,q,l} \sum_{u=0}^{N_s} \sum_{v=0}^{u(M_2-1)} \frac{\mathcal{A}_1 \alpha \sqrt{\varphi} (-1)^u (2\lambda)^\zeta \Gamma(\eta + \zeta)}{2^{\frac{3}{2}} \beta_0^\nu \Gamma(\eta + \frac{1}{2})} \\ &\quad \times \frac{\Gamma(\eta - \zeta) {}_2\mathcal{F}_1\left(\eta + \zeta, \zeta + \frac{1}{2}; \eta + \frac{1}{2}; \frac{\psi - \lambda}{\psi + \lambda}\right)}{(\psi + \lambda)^{\eta + \zeta}} \quad (15) \end{aligned}$$

where \mathcal{A}_1 and $\sum_{a,b,p,q,l}$ are defined in (7a). Furthermore, ψ , η , ζ , and λ depend on the summation variables and are defined as $\psi = (\varphi/2) + (u/\beta_0) + (a/\beta_1) + (p + 1/\beta_2)$, $\eta = M_2 + b + q + v + 1/2$, $\zeta = l - b + 1$, and $\lambda = 2\sqrt{a(p+1)}/\beta_1\beta_2$, respectively.

The CEP can also be expressed in an alternative form [28]

$$P_e|\gamma = \alpha \mathcal{Q}(\sqrt{\varphi\gamma}) = \frac{\alpha}{\pi} \sqrt{\frac{\varphi}{2}} \int_0^\infty \frac{e^{-\gamma(s^2 + \varphi/2)}}{s^2 + \varphi/2} ds. \quad (16)$$

By using the variable transformation $s^2 + \varphi/2 = \varphi/(\gamma + 1)$, the average SER can be written as [28]

$$\begin{aligned} \bar{P}_e &= \frac{\frac{\alpha}{\pi} \sqrt{\frac{\varphi}{2}} \int_0^\infty \mathcal{M}_{\gamma_{\text{eq}}}^{\text{TAS}_{\text{subopt}_j}}(s^2 + \varphi/2)}{s^2 + \varphi/2} ds \\ &= \frac{\frac{\alpha}{2\pi} \int_{-1}^1 \mathcal{M}_{\gamma_{\text{eq}}}^{\text{TAS}_{\text{subopt}_j}}(\varphi/(\gamma + 1))}{\sqrt{1 - \gamma^2}} d\gamma. \quad (17) \end{aligned}$$

Then, we use the accurate and computationally efficient method proposed in [28], which uses the Gauss–Chebyshev approximation [21] to obtain a compact closed-form approximation for the average BER of $\text{TAS}_{\text{subopt}_1}$ and $\text{TAS}_{\text{subopt}_2}$ as follows:

$$\begin{aligned} \bar{P}_e^{\text{TAS}_{\text{subopt}_j}} &\Big|_{j=1}^2 \\ &= \frac{\alpha}{2N_p} \sum_{k=1}^{N_p} \mathcal{M}_{\gamma_{\text{eq}}}^{\text{TAS}_{\text{subopt}_j}}\left(\frac{\varphi}{2} \sec^2(\theta_k)\right) + R_{N_p} \quad (18) \end{aligned}$$

where N_p is a small positive integer, $\theta_k = (2k - 1)\pi/4N_p$, and R_{N_p} is the remainder term. R_{N_p} becomes negligible as N_p increases, even for small values such as 10 (see Section V).

D. High SNR Analysis

To obtain direct system design insights such as diversity order and array gain, the asymptotic outage probability and the average SER are derived for the $\text{TAS}_{\text{subopt}_1}$, $\text{TAS}_{\text{subopt}_2}$, and TAS_{opt} strategies.

1) *Asymptotic Outage Probability*: The cdf of $\gamma_{\text{eq}}^{\text{subopt}_1}$ can be approximated by a single polynomial term for $x \rightarrow 0^+$ as (see Appendix C for the proof)

$$\begin{aligned} F_{\gamma_{\text{eq}}}^{\infty \text{subopt}_1}(x) &= \begin{cases} \Omega_1^{\text{subopt}_1}\left(\frac{x}{\bar{\gamma}}\right)^{d_1^{\text{subopt}_1}} + o\left(x^{d_1^{\text{subopt}_1+1}\right), & m_1 < m_2 N_d \\ \Omega_2^{\text{subopt}_1}\left(\frac{x}{\bar{\gamma}}\right)^{d_2^{\text{subopt}_1}} + o\left(x^{d_2^{\text{subopt}_1+1}\right), & m_1 > m_2 N_d \\ \Omega_3^{\text{subopt}_1}\left(\frac{x}{\bar{\gamma}}\right)^{d_3^{\text{subopt}_1}} + o\left(x^{d_3^{\text{subopt}_1+1}\right), & m_1 = m_2 N_d \end{cases} \quad (19a) \end{aligned}$$

where $\Omega_1^{\text{subopt}_1}$, $\Omega_2^{\text{subopt}_1}$, and $\Omega_3^{\text{subopt}_1}$ are given by

$$\Omega_1^{\text{subopt}_1} = \frac{(m_0/k_0)^{m_0 N_s N_d} (m_1/k_1)^{m_1 N_r} (m_0 N_s N_d)!}{((m_0 N_d)!)^{N_s} (m_0 N_s N_d + m_1 N_r)!} \quad (19b)$$

$$\begin{aligned} \Omega_2^{\text{subopt}_1} &= \frac{(m_0/k_0)^{m_0 N_s N_d} (m_2/k_2)^{m_2 N_r N_d}}{((m_0 N_d)!)^{N_s} ((m_2 N_d)!)^{N_r}} \\ &\quad \times \frac{(m_0 N_s N_d)! (m_2 N_r N_d)!}{(N_d [m_0 N_s + m_2 N_r])!} \quad (19c) \end{aligned}$$

$$\Omega_3^{\text{subopt}_1} = \Omega_1^{\text{subopt}_1} + \Omega_2^{\text{subopt}_1}. \quad (19d)$$

Moreover, $d_1^{\text{subopt}_1}$, $d_2^{\text{subopt}_1}$, and $d_3^{\text{subopt}_1}$ are given by $d_1^{\text{subopt}_1} = m_0 N_s N_d + m_1 N_r$, $d_2^{\text{subopt}_1} = m_0 N_s N_d + m_2 N_r N_d$, and $d_3^{\text{subopt}_1} = m_0 N_s N_d + L_1 N_r$, where L_1 is defined as $L_1 = m_1 = m_2 N_d$. Next, the outage probability of $\text{TAS}_{\text{subopt}_1}$ at high SNRs can be obtained by evaluating (19a) at $x = \gamma_{\text{th}}$ as $P_{\text{out,subopt}_1}^\infty = F_{\gamma_{\text{eq}}}^{\infty \text{subopt}_1}(\gamma_{\text{th}})$.

Similarly, the cdf of $\gamma_{\text{eq}}^{\text{subopt}_2}$ can be approximated by a single polynomial term for $x \rightarrow 0^+$ as (see Appendix E for the proof)

$$\begin{aligned} F_{\gamma_{\text{eq}}}^{\infty \text{subopt}_2}(x) &= \begin{cases} \Omega_1^{\text{subopt}_2}\left(\frac{x}{\bar{\gamma}}\right)^{d_1^{\text{subopt}_2}} + o\left(x^{d_1^{\text{subopt}_2+1}\right), & m_1 N_s < m_2 N_d \\ \Omega_2^{\text{subopt}_2}\left(\frac{x}{\bar{\gamma}}\right)^{d_2^{\text{subopt}_2}} + o\left(x^{d_2^{\text{subopt}_2+1}\right), & m_1 N_s > m_2 N_d \\ \Omega_3^{\text{subopt}_2}\left(\frac{x}{\bar{\gamma}}\right)^{d_3^{\text{subopt}_2}} + o\left(x^{d_3^{\text{subopt}_2+1}\right), & m_1 N_s = m_2 N_d \end{cases} \quad (20a) \end{aligned}$$

where $\Omega_1^{\text{subopt}_2}$, $\Omega_2^{\text{subopt}_2}$, and $\Omega_3^{\text{subopt}_2}$ are given by

$$\Omega_1^{\text{subopt}_2} = \frac{(m_0/k_0)^{m_0 N_d} (m_1/k_1)^{m_1 N_s N_r} (m_0 N_s N_r)!}{((m_1 N_r)!)^{N_s} (m_0 N_d + m_1 N_s N_r)!} \quad (20b)$$

$$\Omega_2^{\text{subopt}_2} = \frac{(m_0/k_0)^{m_1 N_d} (m_2/k_2)^{m_2 N_r N_d} (m_2 N_r N_d)!}{((m_2 N_d)!)^{N_r} (N_d [m_0 + m_2 N_r])!} \quad (20c)$$

$$\Omega_3^{\text{subopt}_2} = \Omega_1^{\text{subopt}_2} + \Omega_2^{\text{subopt}_2}. \quad (20d)$$

TABLE I
DIVERSITY ORDERS OF THE THREE TAS STRATEGIES. $m_0 = m_1 = m_2 = m$

TAS Strategy	Diversity Order			
	$N_s=1$	$N_r=1$	$N_d=1$	$N_s=N_r=N_d=N$
TAS _{opt}	$m(N_r+N_d)$	$m(N_s N_d + \min(N_s, N_d))$	$m(N_s+N_r)$	$2mN^2$
TAS _{subopt₁}	$m(N_r+N_d)$	$m(N_s N_d + 1)$	$m(N_s+N_r)$	$mN(N+1)$
TAS _{subopt₂}	$m(N_r+N_d)$	$m(N_d + \min(N_s, N_d))$	$m(N_r+1)$	$mN(N+1)$

In (20a), $d_1^{\text{subopt}_2}$, $d_2^{\text{subopt}_2}$, and $d_3^{\text{subopt}_2}$ are given by $d_1^{\text{subopt}_2} = m_0 N_d + m_1 N_s N_r$, $d_2^{\text{subopt}_2} = m_0 N_d + m_2 N_r N_d$, and $d_3^{\text{subopt}_2} = m_0 N_d + L_2 N_r$, where L_2 is defined as $L_2 = m_1 N_2 = m_2 N_d$. Next, the outage probability of TAS_{subopt₂} at high SNRs can readily be derived by evaluating (20a) at $x = \gamma_{\text{th}}$ as $P_{\text{out,subopt}_2}^\infty = F_{\gamma_{\text{eq}}^{\text{subopt}_2}}^\infty(\gamma_{\text{th}})$.

Although [5] derives the diversity order of TAS_{opt}, the exact asymptotic outage probability and the average SER analysis, which provide the exact array gains, are still not available in [5]. To this end, the cdf of TAS_{opt} for $x \rightarrow 0^+$ can be approximated by a single polynomial term as (see Appendix F for the proof)

$$F_{\gamma_{\text{eq}}}^\infty(x) = \begin{cases} \Omega_1^{\text{opt}} \left(\frac{x}{\bar{\gamma}}\right)^{d_1^{\text{opt}}} + o\left(x^{d_1^{\text{opt}}+1}\right), & m_1 N_s < m_2 N_d \\ \Omega_2^{\text{opt}} \left(\frac{x}{\bar{\gamma}}\right)^{d_2^{\text{opt}}} + o\left(x^{d_2^{\text{opt}}+1}\right), & m_1 N_s > m_2 N_d \\ \Omega_3^{\text{opt}} \left(\frac{x}{\bar{\gamma}}\right)^{d_3^{\text{opt}}} + o\left(x^{d_3^{\text{opt}}+1}\right), & m_1 N_s = m_2 N_d \end{cases} \quad (21a)$$

where Ω_1^{opt} , Ω_2^{opt} , and Ω_3^{opt} are given by

$$\Omega_1^{\text{opt}} = \frac{(m_0/k_0)^{m_0 N_s N_d} (m_1/k_1)^{m_1 N_s N_r}}{((m_0 N_d)!(m_1 N_r)!)^{N_s}} \times \frac{(m_1 N_s N_r)!(m_0 N_s N_d)!}{(m_0 N_s N_d + m_1 N_s N_r)!} \quad (21b)$$

$$\Omega_2^{\text{opt}} = \frac{(m_0/k_0)^{m_0 N_s N_d} (m_2/k_2)^{m_2 N_r N_d}}{((m_0 N_d)!(m_2 N_d)!)^{N_s}} \times \frac{(m_2 N_r N_d)!(m_0 N_s N_d)!}{(m_0 N_s N_d + m_2 N_r N_d)!} \quad (21c)$$

$$\Omega_3^{\text{opt}} = \Omega_1^{\text{opt}} + \Omega_2^{\text{opt}}. \quad (21d)$$

Furthermore, in (21a), d_1^{opt} , d_2^{opt} , and d_3^{opt} are defined by $d_1^{\text{opt}} = m_0 N_s N_d + m_1 N_s N_r$, $d_2^{\text{opt}} = m_0 N_s N_d + m_2 N_r N_d$, and $d_3^{\text{opt}} = m_0 N_s N_d + L_3 N_r$, where $L_3 = m_1 N_s = m_2 N_d$. Now, the asymptotic outage probability of TAS_{opt}, which is exact at high SNRs, can readily be derived by evaluating (21a) at $x = \gamma_{\text{th}}$ as $P_{\text{out,opt}}^\infty = F_{\gamma_{\text{eq}}^{\text{opt}}}^\infty(\gamma_{\text{th}})$.

2) *Asymptotic Average SER*: The asymptotic average SER of TAS_{subopt₁} and TAS_{subopt₂} can readily be derived by substituting (19a) and (20a) into the integral representation of SER in Section IV-C as follows:

$$P_{e,\text{TASsubopt}_i}^\infty = \frac{\Omega_j^{\text{subopt}_i} \alpha 2^{d_j^{\text{subopt}_i} - 1} \Gamma\left(d_j^{\text{subopt}_i} + \frac{1}{2}\right)}{\sqrt{\pi}(\varphi\bar{\gamma})^{d_j^{\text{subopt}_i}}} + o\left(\bar{\gamma}^{-\left(d_j^{\text{subopt}_i}+1\right)}\right) \quad (22)$$

where $i = 1, 2$ stands for each suboptimal TAS strategy, and $j = 1, 2, 3$ represents each case in (19a) and (20a). Similarly, the asymptotic average SER of TAS_{opt} can readily be obtained by replacing $\Omega_j^{\text{subopt}_i}$ and $d_j^{\text{subopt}_i}$ in (22) by $\Omega_j^{\text{opt}}|_{j=1}^3$ and $d_1^{\text{opt}}|_{j=1}^3$ defined in (21a).

3) *Diversity Order and Array Gain*: In the high SNR regime, the average SER can be represented by $P_e^\infty \approx [G_a \bar{\gamma}]^{-G_d}$, where G_d and G_a are referred to as the diversity and array gains, respectively [29].

TAS_{opt} has been shown to provide the maximum achievable diversity order (G_d) of cooperative MIMO AF relay networks. Thus, the G_d of TAS_{opt} over Rayleigh fading is given by $G_d^{\text{TASopt}} = N_s N_d + N_r \min(N_s, N_d)$ [5]. This result can readily be extended for Nakagami- m fading by using our asymptotic average SER of TAS_{opt} in Section IV-D as follows:

$$G_d^{\text{TASopt}} = m_0 N_s N_d + N_r \min(m_1 N_s, m_2 N_d). \quad (23)$$

By following (19a), (20a), and (22), the G_d of TAS_{subopt₁} and TAS_{subopt₂} can be written as

$$G_d^{\text{TASsubopt}_1} = m_0 N_s N_d + N_r \min(m_1, m_2 N_d) \quad (24)$$

$$G_d^{\text{TASsubopt}_2} = m_0 N_d + N_r \min(m_1 N_s, m_2 N_d). \quad (25)$$

Similarly, the array gains of TAS_{subopt₁} and TAS_{subopt₂} can readily be obtained by substituting (22) into $G_a = ((P_e^\infty)^{-1/G_d} / \bar{\gamma})$.

In Table I, the G_d of each TAS strategy over symmetric Nakagami- m fading (i.e., $m_0 = m_1 = m_2 = m$) is presented for several special cases to obtain valuable insights. For example, when S has only one antenna ($N_s = 1$), all three strategies achieve the same diversity order. Moreover, if D has only one antenna ($N_d = 1$), then TAS_{opt} and TAS_{subopt₁} provide the same diversity order. Thus, TAS_{subopt₁} is preferred over TAS_{opt} whenever $N_d = 1$. When the number of antennas at each node is the same, the G_d provided by the both TAS_{subopt₁} and TAS_{subopt₂} is identical. In practice, the direct channel may be completely unavailable due to heavy shadowing. In this case, the diversity orders of the three strategies are given by $G_d^{\text{TASopt}} = G_d^{\text{TASsubopt}_2} = N_r \min(m_1 N_s, m_2 N_d)$ and $G_d^{\text{TASsubopt}_1} = N_r \min(m_1, m_2 N_d)$. Thus, TAS_{subopt₂} is a preferable choice than the others since it always provides a better G_d than TAS_{subopt₁} and the same G_d as TAS_{opt}.

E. Performance Analysis Without the Direct Path

In dual-hop MIMO AF relaying, when the direct path is not taken into account [13], the optimal TAS strategy is to select

the antenna indices I and K at S and R to maximize the SNRs of the $S \rightarrow R$ and $R \rightarrow D$ channels as (5) in Remark III.1.

The cdf and the mgf of the e2e SNR of the optimal TAS for dual-hop MIMO AF relaying, when the direct path is ignored, are given by (45) and (12a). Moreover, the average SER can be derived by substituting (45) into the integral representation of \bar{P}_e in Section IV-C and by using [20, eq. (6.621.3)] as follows:

$$\bar{P}_e = \frac{\alpha}{2} - \frac{\alpha}{2} \sqrt{\frac{\varphi}{2}} \sum_{p,q,a,b,c} \frac{\mathcal{A}_4(2\epsilon)^\nu \Gamma(\mu + \nu) \Gamma(\mu - \nu)}{\Gamma(\mu + \frac{1}{2})} \times \frac{{}_2\mathcal{F}_1\left(\mu + \nu, \nu + \frac{1}{2}; \mu + \frac{1}{2}; \frac{\frac{\varphi}{2} + \delta - \epsilon}{\frac{\varphi}{2} + \delta + \epsilon}\right)}{\left(\frac{\varphi}{2} + \delta + \epsilon\right)^{\mu + \nu}} \quad (26a)$$

where \mathcal{A}_4 is given by

$$\mathcal{A}_4 = \frac{2N_s \binom{N_r}{p} \binom{N_s-1}{c} (M_1+q+b-1) (-1)^{p+q+1} p^{\binom{c-q+1}{2}}}{\Gamma(M_1)(a+1)^{\frac{c-q+1}{2}}} \times \frac{\phi_{q,p,M_2} \phi_{b,a,M_1}}{\beta_1^{\frac{2M_1+2b+q-c-1}{2}} \beta_2^{\frac{c+q+1}{2}}}. \quad (26b)$$

In (26a), $\sum_{p,q,a,b,c} = \sum_{p=1}^{N_r} \sum_{q=0}^{p(M_2-1)} \sum_{a=0}^{N_s-1} \sum_{b=0}^{a(M_1-1)}$. Furthermore, μ , ν , δ , and ϵ depend on the summation variables and are defined as $\mu = M_1 + b + q + 1/2$, $\nu = l - q + 1$, $\delta = (a + 1/\beta_1) + (p/\beta_2)$, and $\epsilon = 2\sqrt{p(a+1)/\beta_1\beta_2}$, respectively.

The asymptotic outage probability is given by (46), and the asymptotic average SER can readily be obtained by using (46) and (22). The diversity order is given by $G_d = N_r \min(m_1 N_s, m_2 N_d)$. These results are also novel.

F. Feedback Delay Effect on the Performance of TAS for Dual-Hop MIMO AF Relay Networks

In practice, the transmit antennas could be selected by using outdated CSI due to feedback delays. Thus, in this section, the impact of feedback delays on the system performance of TAS strategies for dual-hop MIMO relay networks is studied.

In practical systems, the feedback channel from the receiver to the transmitter experiences delays. We thus assume that the transmit antennas at S and R are selected based on the outdated CSI received via feedback channels of $S \rightarrow D$, $S \rightarrow R$, and $R \rightarrow D$ having τ_0 , τ_1 , and τ_2 time delays, respectively. These three channels can be modeled as [30], [31]

$$\mathbf{H}_i(t)|_{t=0}^2 = \rho_i \mathbf{H}_i(t - \tau_i) + \mathbf{E}_{d,i} \quad (27)$$

where ρ_i is the normalized correlation coefficients between $h_i^{i,j}(t)$ and $h_i^{i,j}(t - \tau_i)$. For Clarke's fading spectrum, $\rho_i = \mathcal{J}_0(2\pi f_i \tau_i)$, where f_i is the Doppler fading bandwidth. Further, $\mathbf{E}_{d,i}$ is the error matrix, which is incurred by feedback delay, having mean zero and variance $(1 - \rho_i^2)$ Gaussian entries.

1) *Feedback Delay Effect on the Performance of TAS_{opt} When the Direct Path Is Ignored:* In the first time slot, S selects the I th transmit antenna based on the CSI received by the local $R \rightarrow S$ feedback channel, which is assumed to experience a

time delay τ_1 . Similarly, in the second time slot, the relay R selects the K th transmit antenna based on the τ_2 -delayed CSI.

Under this channel model, the exact cdf of the e2e SNR can be derived as (see Appendix G for the proof)

$$F_{\gamma_{\text{eq}}^{\text{opt}}}(x) = 1 - \sum_{a,b,k,l} \sum_{p,q,u,v} \beta_1^b \beta_2^q \rho_1^k (1 - \rho_1)^{b-k} \times \rho_2^u (1 - \rho_2)^{q-u} \Psi \Phi^{\frac{2b+v+l+1}{2}} \Theta^{\frac{2(M_2+q+u)+v-l+1}{2}} \times x^{M_2+u+l} e^{-(\Phi+\Theta)x} \mathcal{K}_{v-l+1}\left(2x\sqrt{\Phi\Theta}\right) \quad (28a)$$

where Ψ , Φ , and Θ depend on the summation variables and are defined as

$$\Psi = \frac{2(-1)^{a+p} N_s N_r \binom{N_s-1}{a} \binom{N_r-1}{p} \binom{b}{k} \binom{q}{u} (M_2+u+l-1)}{\Gamma(M_1)\Gamma(M_2)\Gamma(M_2+u)(l)!} \times \frac{\phi_{b,a,M_1} \phi_{q,b,M_2} \Gamma(M_1+b)\Gamma(M_2+q)}{(a+1)^{M_1+b+k} (p+1)^{M_2+q+u}} \quad (28b)$$

$$\Phi = \frac{a+1}{\beta_1(1+a(1-\rho_1))} \quad \text{and} \quad \Theta = \frac{p+1}{\beta_2(1+p(1-\rho_2))}. \quad (28c)$$

Moreover, the two summations in (28a) are defined as $\sum_{a,b,k,l} = \sum_{a=0}^{N_s-1} \sum_{b=0}^{a(M_1-1)} \sum_{k=0}^b \sum_{l=1}^{M_1+k-1}$ and $\sum_{p,q,u,v} = \sum_{p=0}^{N_r-1} \sum_{q=0}^{p(M_2-1)} \sum_{u=0}^q \sum_{v=0}^{M_2+u+l-1}$. Now, the exact outage probability can readily be obtained by using evaluation (28a) at γ_{th} .

The average SER for the outdated CSI case can readily be derived by substituting (28a) into the integral representation of \bar{P}_e in Section IV-C and evaluating the integral by using [20, eq. (6.621.3)] as follows:

$$\bar{P}_e = \frac{\alpha}{2} - \alpha \sqrt{\varphi} \sum_{a,b,k,l} \sum_{p,q,u,v} \rho_1^k (1 - \rho_1)^{b-k} \rho_2^u (1 - \rho_2)^{q-u} \times \frac{2^{v-l-\frac{1}{2}} \Psi \Phi^{b+v+1} \Theta^{M_2+q+u+v-l+1} \beta_1^b \beta_2^q \Gamma(\mu + \nu)}{\Gamma(\mu + \frac{1}{2})} \times \frac{\Gamma(\mu - \nu) {}_2\mathcal{F}_1\left(\mu + \nu, \nu + \frac{1}{2}; \mu + \frac{1}{2}; \frac{\frac{\varphi}{2} + \delta - \epsilon}{\frac{\varphi}{2} + \delta + \epsilon}\right)}{\left(\frac{\varphi}{2} + \delta + \epsilon\right)^{\mu + \nu}} \quad (29)$$

where μ , ν , δ , and ϵ depend on the summation variables and are defined as $\mu = M_2 + u + l + 1/2$, $\nu = v - l + 1$, $\delta = \Phi + \Theta$, and $\epsilon = 2\sqrt{\Phi\Theta}$, respectively.

By following similar steps to those in Appendices A and G, the upper bounds for the outage and average SER of TAS_{opt}, when the direct path is considered, can be derived. Similarly, the exact outage and the average SER of TAS_{subopt1} and TAS_{subopt2} can be derived as well. However, for the sake of brevity, these results are omitted.

2) *High SNR Performance Metrics When the Antenna Selection Is Based on Outdated CSI:* To quantify the amount of performance degradation in terms of reduction in diversity order and array gain, when the transmit antennas at S , R , and D

are selected based on the outdated CSI, the asymptotic outage probability and the average SER of TAS_{opt} are derived.

Case I: When the direct path is considered, the cdf of the e2e SNR can be approximated by a single polynomial term for $x \rightarrow 0^+$ as

$$F_{\gamma_{eq}}^{\infty}(x) = \begin{cases} \Phi_1 \left(\frac{x}{\bar{\gamma}} \right)^{d_0+d_1} + o(x^{d_0+d_1+1}), & m_1 N_r < m_2 N_d \\ \Phi_2 \left(\frac{x}{\bar{\gamma}} \right)^{d_0+d_2} + o(x^{d_0+d_2+1}), & m_1 N_r > m_2 N_d \\ \Phi_3 \left(\frac{x}{\bar{\gamma}} \right)^{d_0+d_3} + o(x^{d_0+d_3+1}), & m_1 N_r = m_2 N_d \end{cases} \quad (30a)$$

where $\Phi_j|_{j=1}^3$ is given as

$$\Phi_j = \frac{\Delta_0 \Delta_j \Gamma(d_0 + 1) \Gamma(d_j + 1)}{\Gamma(d_0 + d_j + 1)}, \quad \text{for } j = 1, 2, 3. \quad (30b)$$

Further, Δ_0 , Δ_1 , Δ_2 , and Δ_3 are defined as

$$\Delta_j|_{j=0}^2 = \sum_{a=0}^{N_j-1} \sum_{b=0}^{a(M_j-1)} \frac{N_j m_j^{M_j} \binom{N_j-1}{a} (-1)^a \phi_{b,a,M_j} \Gamma(M_j+b)}{M_j k_j^{M_j} \Gamma^2(M_j)} \times \frac{(1-\rho_j)^b}{(1+a(1-\rho_j))^{M_j+b}}, \quad \text{for } j = 0, 1, 2 \quad (30c)$$

$$\Delta_3 = \Delta_1 + \Delta_2. \quad (30d)$$

In (30c), $N_0 = N_1 = N_s$, and $N_2 = N_r$. Furthermore, in (30a), $d_0 = m_0 N_d$, $d_1 = m_1 N_r$, $d_2 = m_2 N_d$, and $d_3 = m_2 N_d = m_1 N_s$. Here, $\rho_j|_{j=0}^2 = \mathcal{J}_0(2\pi B_{f_j} \tau_j)$, where $B_{f_j}|_{j=0}^2$ is the Doppler fading frequency, and $\tau_j|_{j=0}^2$ is the time delay for the $S \rightarrow D$, $S \rightarrow R$, and $R \rightarrow D$ feedback channels, respectively.

Case II: When the direct path is ignored, the cdf of the e2e SNR can be approximated by a single polynomial term for $x \rightarrow 0^+$ as

$$F_{\gamma_{eq}}^{\infty}(x) = \begin{cases} \Phi'_1 \left(\frac{x}{\bar{\gamma}} \right)^{d_1} + o(x^{d_1+1}), & m_1 N_r < m_2 N_d \\ \Phi'_2 \left(\frac{x}{\bar{\gamma}} \right)^{d_2} + o(x^{d_2+1}), & m_1 N_r > m_2 N_d \\ \Phi'_3 \left(\frac{x}{\bar{\gamma}} \right)^{d_3} + o(x^{d_3+1}), & m_1 N_r = m_2 N_d \end{cases} \quad (31)$$

where $\Phi'_1 = \Delta_1$, $\Phi'_2 = \Delta_2$, and $\Phi'_3 = \Delta_1 + \Delta_2$. Here, d_1 , d_2 , and d_3 are same as in (30a).

The asymptotic outage probability, which is exact at high SNRs, for both of the above cases can be obtained by evaluating the corresponding cdfs at γ_{th} . The proofs of (30a) and (31) follow similar steps to those in Appendix B and omitted for the sake of brevity.

The asymptotic average SER can readily be obtained by using $P_e^{\infty} = (\Phi \alpha 2^{G_d-1} \Gamma(G_d+1/2) / \sqrt{\pi} (\varphi \bar{\gamma})^{G_d}) + o(\bar{\gamma}^{-(G_d+1)})$. When the direct path is considered, the diversity order is given by $G_d = m_0 N_d + \min(m_1 N_r, m_2 N_d)$, and Φ is defined in (30a) as Φ_1 , Φ_2 , and Φ_3 for the three cases $m_1 N_s < m_2 N_d$, $m_1 N_s = m_2 N_d$, and $m_1 N_s > m_2 N_d$, respectively. Similarly, when the direct path is ignored, the

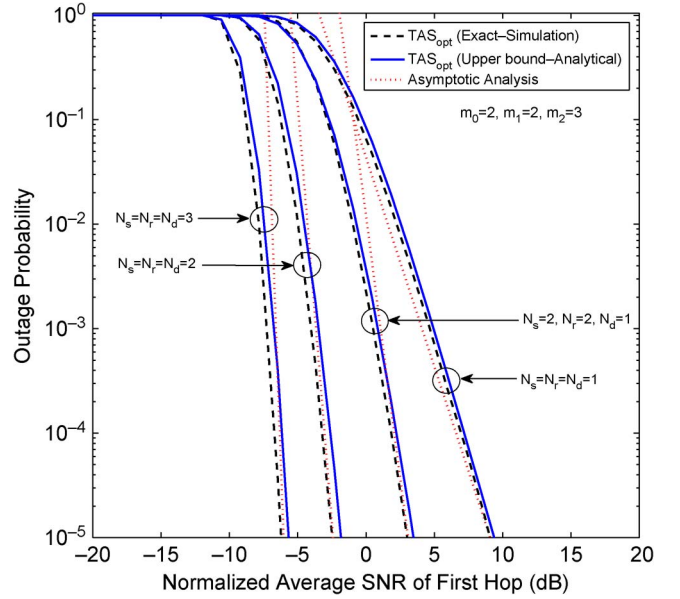


Fig. 2. Outage probability of TAS_{opt} for AF MIMO relay networks. The direct path is considered. The distances are $l_1 = l_0/3$ and $l_2 = 2l_0/3$, and the path loss exponent is $\varpi = 2.5$.

diversity order is given by $G_d = \min(m_1 N_r, m_2 N_d)$, and Φ is defined as Φ'_1 , Φ'_2 , and Φ'_3 in (31).

3) *Amount of Performance Degradation Due to Outdated CSI*: In this section, the amount of performance degradation of TAS_{opt} due to feedback delay is quantified. The diversity order reduction of TAS_{opt} due to the feedback delay effect over the perfect CSI can be derived by using our high SNR analysis in Sections IV-D and F2 as follows: For case I (with the direct path), the diversity order reduction is $G_d^R = m_0 N_d (N_s - 1) + N_r \min(m_1 N_s, m_2 N_d) - \min(m_1 N_r, m_2 N_d)$. The array gain is degraded by a factor $\Omega_j^{\text{opt}} / \Phi_j|_{j=1}^3$, where Ω_j^{opt} and Φ_j are defined in (21a) and (30a), respectively. Similarly, for case II (without direct path), the reduction of diversity order is given by $G_d^R = N_r \min(m_1 N_s, m_2 N_d) - \min(m_1 N_r, m_2 N_d)$.

V. NUMERICAL RESULTS

This section verifies our analysis through Monte Carlo simulations. To capture the effect of the network geometry, the average SNR of the i th hop is modeled by $\bar{\gamma}_i|_{i=1}^2 = \bar{\gamma}_0 (l_0/l_i)^\varpi$, where $\bar{\gamma}_0$ is the average SNR of the direct path, and ϖ is the path loss exponent. The distances between the terminals $S \rightarrow D$, $S \rightarrow R$, and $R \rightarrow D$ are denoted by l_0 , l_1 , and l_2 , respectively.

1) *Outage Probability of TAS_{opt}* : In Fig. 2, the exact outage probability of TAS_{opt} , which is obtained via Monte Carlo simulations, is compared with our outage upper bound (7a) for several antenna configurations. Our outage upper bound is just a fraction of a decibel off of the exact. The asymptotic outage curves are plotted to obtain direct insights about the diversity order and array gain. Thus, the bound provides accurate insights about the important system parameters, such as the diversity order, and can be used as a benchmark to design practical MIMO TAS relay networks.

2) *Average BER of TAS_{opt}* : Similarly, in Fig. 3, the closed-form upper bound for the average BER of BPSK for TAS_{opt} is

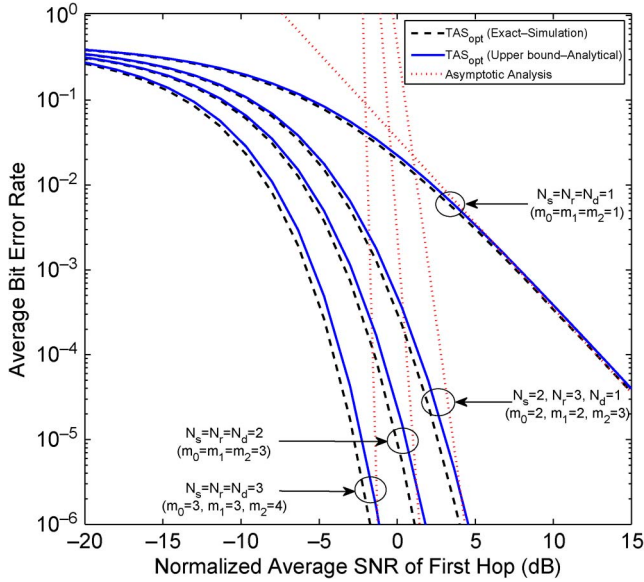


Fig. 3. Average BER of BPSK of TAS_{opt} for AF MIMO relay networks. The direct path is considered. The distances are $d_1 = l_0/3$ and $d_2 = 2l_0/3$, and the path loss exponent is $\varpi = 2.5$.

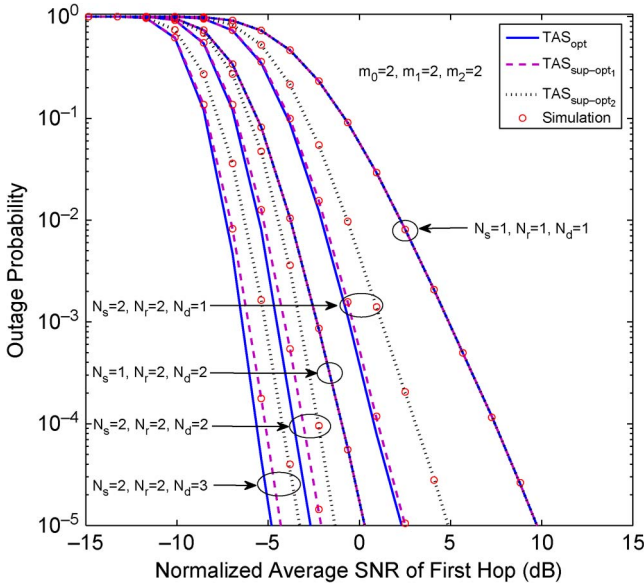


Fig. 4. Outage probability of TAS_{opt} , TAS_{subopt_1} , and TAS_{subopt_2} strategies for AF MIMO relay networks. The direct path is considered. The distances are $l_1 = l_2 = l_0$, and the path loss exponent is $\varpi = 2.5$.

compared for different antenna configurations when the direct path is considered. Fig. 3 also shows the tightness of our BER bound for different fading parameters (i.e., m_0 , m_1 , and m_2). Similar to the outage bound, the BER bound is always exact within 1 dB and predicts the diversity order accurately. The asymptotic BER curves are plotted to obtain valuable system-design insights, such as diversity order and array gain.

3) *Outage Probability Comparison:* Fig. 4 shows the outage probability of the three TAS strategies for several antenna setups. Here, the three nodes are placed in the vertices of an equilateral triangle. Further, all the channels experience the same severity of fading (when $m_0 = m_1 = m_2 = 2$). The exact outage probability of TAS_{opt} is computed by using

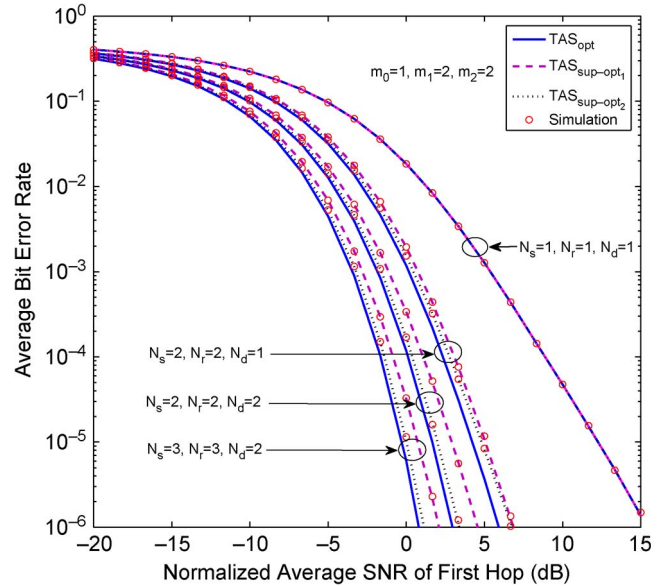


Fig. 5. Average BER of TAS_{opt} , TAS_{subopt_1} and TAS_{subopt_2} strategies for AF MIMO relay networks. The direct path is considered. The distances are $l_1 = 3l_0/7$ and $l_2 = 4l_0/7$, and the path loss exponent is $\varpi = 2.5$.

Monte Carlo simulations, whereas those of TAS_{subopt_1} and TAS_{subopt_2} are obtained by using (14) with $R_{N_p} = 20$. The outage probability of a relay network with single-antenna nodes (i.e., $N_s = N_r = N_d = 1$) is also plotted as a benchmark to illustrate the performance gain obtained by TAS for AF MIMO relaying. The following conclusions can be drawn from Fig. 4.

- 1) As expected, TAS_{opt} always performs better than TAS_{subopt_1} and TAS_{subopt_2} for the given antenna setups, at the expense of higher implementation complexity.
- 2) TAS_{subopt_1} performs very close to TAS_{opt} in terms of outage when D is equipped with a single antenna. TAS_{subopt_1} is thus a better choice than TAS_{opt} for networks with $N_d = 1$.
- 3) Under this system setup, TAS_{subopt_1} always performs better than TAS_{subopt_2} . This behavior is well explained because the $S \rightarrow D$ channel is strong, compared with those of $S \rightarrow R$ and $R \rightarrow D$, and the performance of TAS_{subopt_1} is dominated by the $S \rightarrow D$ channel.
- 4) Fig. 4 also shows the impact of the number of antennas at D on the outage probability for a fixed number of antennas at S and R . Whenever S is equipped with a single antenna, the performance of the three TAS strategies is identical. This insight thus shows that any of the three strategies can effectively be used for $S \rightarrow R \rightarrow D$ uplink, where S is usually a mobile device equipped with a single antenna due to power and space constraints.
- 5) Similarly, TAS_{subopt_1} can be used instead of TAS_{opt} for the $D \rightarrow R \rightarrow S$ downlink as both of them provide the same diversity order whenever $N_d = 1$.

These observations/insights can also be verified through asymptotic analysis in Section IV-D. The Monte Carlo simulation results agree well with our closed-form outage probability approximation.

4) *Average BER Comparison:* Similarly, Fig. 5 compares the average BER of the BPSK of the three TAS strategies, taking

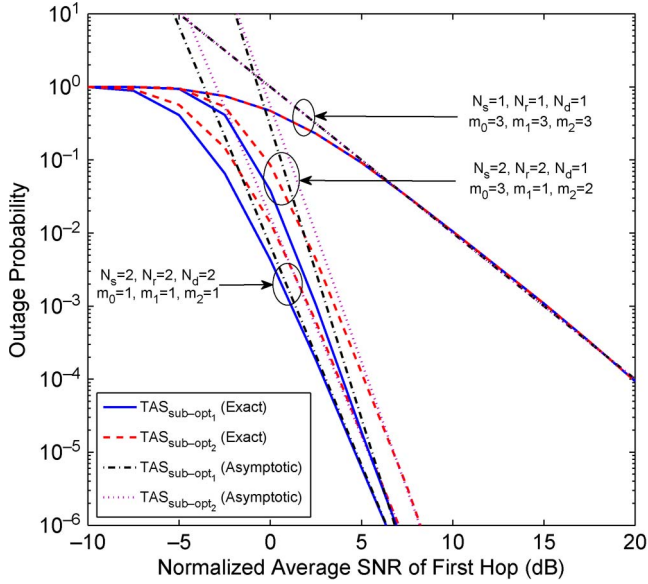


Fig. 6. Asymptotic outage probability of the two suboptimal TAS strategies. The direct path is considered. The distances are $l_0 = l_1 = l_2$, and the path loss exponent is $\varpi = 2.5$.

into account an asymmetric relay network, where $l_1 = 3l_0/7$, and $l_2 = 4l_0/7$. Further, the $S \rightarrow D$, $S \rightarrow R$, and $R \rightarrow D$ channels undergo dissimilar severities of fading (with $m_0 = 1$, $m_1 = 2$, and $m_2 = 2$). The exact average BER of TAS_{opt} is again computed by using Monte Carlo simulation, whereas those of TAS_{subopt_1} and TAS_{subopt_2} are computed by using (18) with $R_{N_p} = 10$. As expected, TAS_{opt} outperforms the other TAS strategies in terms of BER. Contradictory to what we observed in the case of the outage probability, under this system setup, TAS_{subopt_2} always performs better than TAS_{subopt_1} . This behavior can be explained as follows: The system setup consists of a stronger $S \rightarrow R$ channel than the $S \rightarrow D$, and the performance of TAS_{subopt_2} is dominated by the $S \rightarrow R$ channel. We thus obtain the valuable system-design insight that the performance of suboptimal TAS strategies heavily depends upon the strength of $S \rightarrow D$ and $S \rightarrow R$ channels. Under a stronger $S \rightarrow D$ channel, TAS_{subopt_1} performs better than TAS_{subopt_2} , whereas TAS_{subopt_2} outperforms TAS_{subopt_1} whenever the $S \rightarrow R$ channel is stronger. Moreover, the exact agreement between the Monte Carlo simulation points and the analytical results verifies the accuracy of our closed-form average BER approximations.

5) *Verification of the High SNR Analysis*: Fig. 6 shows the exact and asymptotic outage probability of TAS_{subopt_1} and TAS_{subopt_2} . The exact outage curves are from (14), and the asymptotic outage curves are from (19a) and (20a). The exact agreement of the exact and asymptotic outage curves verifies the accuracy of our high SNR analysis. Further, the exact average SER in (18) can also be compared with our asymptotic SER derived in (22). However, for the sake of brevity, this comparison is omitted.

6) *Impact of Outdated CSI on the Outage Probability and Average SER*: In Figs. 7 and 8, the impact of outdated CSI due to feedback delay on the outage probability of TAS_{opt} is shown. Two system scenarios, i.e., 1) without the direct path

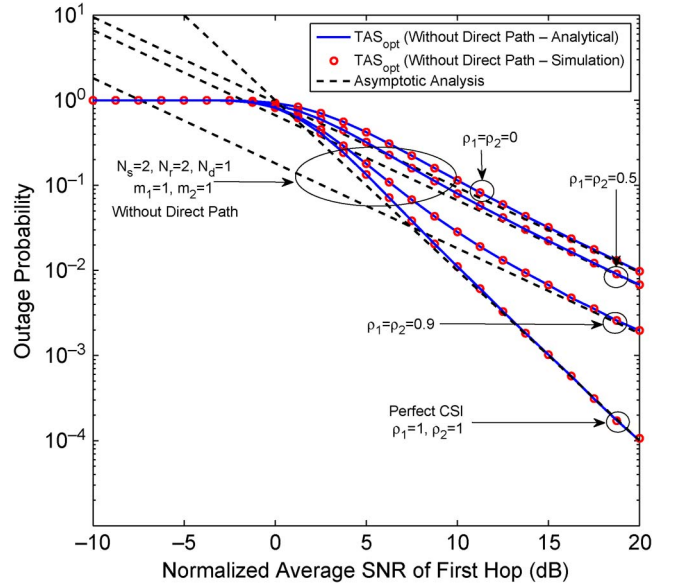


Fig. 7. Impact of outdated CSI on the outage performance of TAS_{opt} for MIMO relaying. The direct path is not considered. The distances are $l_1 = l_2 = l_0/2$, and the path loss exponent is $\varpi = 2.5$.

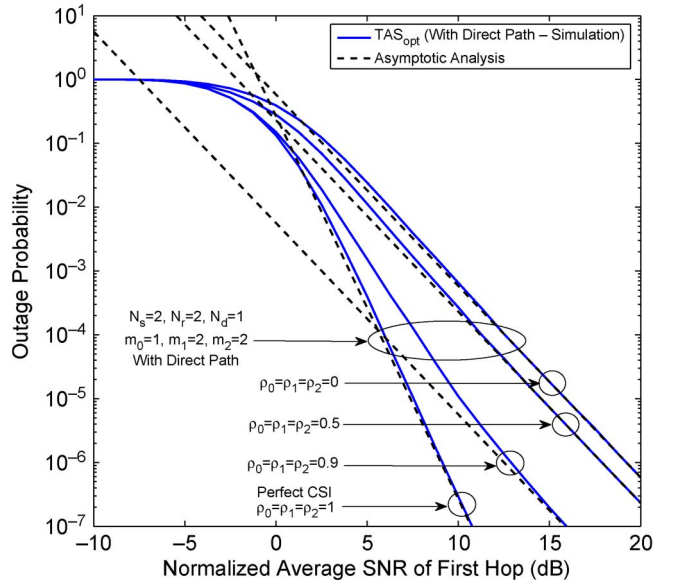


Fig. 8. Impact of outdated CSI on the outage performance of TAS_{opt} for MIMO relaying. The direct path is considered. The distances are $l_1 = l_2 = l_0/2$, and the path loss exponent is $\varpi = 2.5$.

and 2) with the direct path, are treated. The exact outage curves of the former scenario is plotted in Fig. 7 by using the closed-form outage expression in (28a), whereas the outage curves corresponding to the latter scenario are plotted in Fig. 8 by using Monte Carlo simulations. The TAS at S and R is based on the outdated CSI received via the local feedbacks $D \rightarrow S$, $R \rightarrow S$, and $D \rightarrow R$ having time delays τ_0 , τ_1 , and τ_2 , respectively. Several outage curves are obtained by changing ρ_0 , ρ_1 , and ρ_2 , where ρ_l is related to τ_l by following Clarke's fading model; $\rho_l|_{l=0}^2 = \mathcal{J}_0(2\pi B_{f_l} \tau_l)$, where B_{f_l} is the Doppler fading frequency. The two extreme cases $\rho_l = 1$ and $\rho_l = 0$ correspond to the perfect and fully outdated CSI cases. To obtain valuable insights, the asymptotic outage curves are plotted as by using

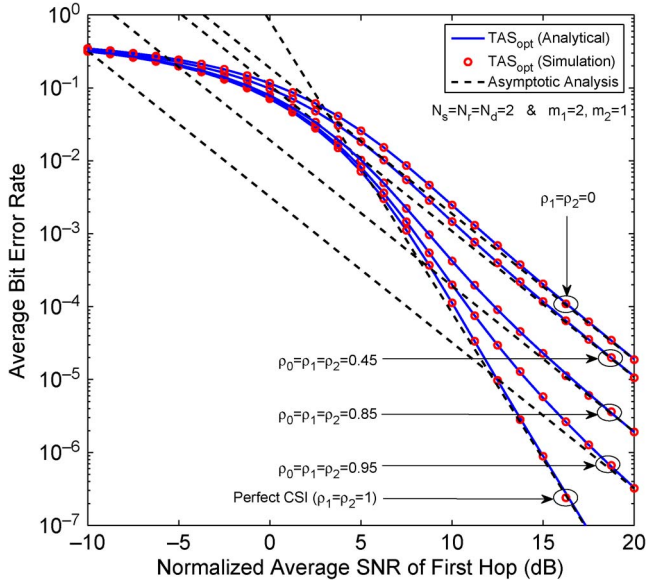


Fig. 9. Impact of outdated CSI on the average BER of BPSK of TAS_{opt} for MIMO relaying. Direct path is not considered. The distances are $l_1 = l_2 = l_0/2$, and the path loss exponent is $\varpi = 2.5$.

(30a) and (31) for both scenarios. Figs. 7 and 8 show that with even a slight time delay in the feedback channel, the diversity order of the system reduces to $G_d = \min(m_1 N_r, m_2 N_d)$ from the full diversity order $G_d = N_r \min(m_1 N_s, m_2 N_d)$. Thus, the outdated CSI has a significant detrimental effect on the outage performance.

Similarly, in Fig. 9, the feedback delay effect on the average BER of BPSK of TAS_{opt} , when the direct path is ignored, is shown. The asymptotic SER curves are plotted to depict the reduction of the diversity order and array gain due to feedback delay. Just as in outage probability case, the feedback delay in TAS has a severe detrimental effect on the average BER.

VI. CONCLUSION

The performance of three TAS strategies for dual-hop MIMO ideal CA-AF relay networks has been analyzed. An upper bound of the cdf of the e2e SNR was derived and used to obtain the upper bounds of the outage probability and the average SER for TAS_{opt} . The exact mgfs of the e2e SNR of TAS_{subopt_1} and TAS_{subopt_2} were derived. Closed-form approximations and asymptotic metrics for the outage probability and the average SER were obtained. The diversity orders of the TAS strategies were summarized to provide valuable insights. Both exact and asymptotic performance metrics are derived for optimal TAS when the direct path is ignored. Our numerical results showed that the choice between TAS_{subopt_1} and TAS_{subopt_2} depends upon the availability of stronger $S \rightarrow D$ or $S \rightarrow R$ channels, and the suboptimal TAS strategies closely perform to the optimal TAS strategy, while retaining significant implementation simplicity than the optimal TAS. Further, our results proved that the TAS based on the outdated CSI incurs significant performance losses. Monte Carlo simulations were provided to validate the accuracy of our analytical developments. Our results clearly provide valuable insights and show that MIMO TAS AF relaying achieves significant performance gains.

APPENDIX A

PROOF OF THE cdf OF A LOWER BOUND OF THE e2e SNR FOR TAS_{opt}

In TAS_{opt} , the antenna indexes I and K are selected at S and R , respectively, according to (6). The upper bound for the cdf of the e2e SNR, i.e., TAS_{opt} , can be derived as

$$\begin{aligned} F_{\gamma_{eq}^{opt}}(x) &= P\left(\max_{1 \leq i \leq N_s} \gamma_{eq}^{(i,K)} \leq x\right) \\ &= P\left(\max_{1 \leq i \leq N_s} \left\{\gamma_{SD}^{(i)} + \gamma_{SRD}^{(i,K)}\right\} \leq x\right) \\ &\leq P\left(\max_{1 \leq i \leq N_s} \left\{\gamma_{SD}^{(i)} \cdot \gamma_{SRD}^{(i,K)}\right\} \leq x\right) \end{aligned} \quad (32)$$

where $\gamma_{SRD}^{(i,K)} = (\gamma_{SR}^{(i)} \gamma_{RD}^{(K)}) / (\gamma_{SR}^{(i)} + \gamma_{RD}^{(K)})$. The probability in (32), i.e., $P(\max_{1 \leq i \leq N_s} \{\gamma_{SD}^{(i)}, \gamma_{SRD}^{(i,K)}\} \leq x)$, can further be lower bounded by $F_{\gamma_{SD}^{(I)}}(x) F_{\gamma_{SRD}^{(I,K)}}(x)$, where $F_{\gamma_{SD}^{(I)}}(x) = P(\max_{1 \leq i \leq N_s} \gamma_{SD}^{(i)} \leq x)$, and $F_{\gamma_{SRD}^{(I,K)}}(x) = P(\max_{1 \leq i \leq N_s} \gamma_{SRD}^{(i,K)} \leq x)$. The cdf of $\gamma_{SD}^{(I)}$ is given by

$$\begin{aligned} F_{\gamma_{SD}^{(I)}}(x) &= \left[1 - e^{-\frac{x}{\beta_0}} \sum_{t=0}^{M_0-1} \frac{1}{t!} \left(\frac{x}{\beta_0}\right)^t\right]^{N_s} \\ &= \sum_{u=0}^{N_s} \sum_{v=0}^{u(M_0-1)} \binom{N_s}{u} \frac{(-1)^u \phi_{v,u,M_0}}{(\beta_0)^v} x^v e^{-\frac{ux}{\beta_0}} \end{aligned} \quad (33)$$

where $M_0 = m_o N_d$, and ϕ_{n,m,M_0} is given by (8). The $F_{\gamma_{SRD}^{(I,K)}}(x)$ is written as

$$\begin{aligned} F_{\gamma_{SRD}^{(I,K)}}(x) &= \int_0^\infty P\left(\max_{1 \leq i \leq N_s} \left\{\frac{\gamma_{SR}^{(i)} \lambda}{\gamma_{SR}^{(i)} + \lambda}\right\} \leq x\right) f_{\gamma_{RD}^{(K)}}(\lambda) d\lambda \\ &= F_{\gamma_{RD}^{(K)}}(x) + \int_0^\infty F_{\gamma_{SR}^{(I)}}\left(\frac{x(x+\lambda)}{\lambda}\right) f_{\gamma_{RD}^{(K)}}(\lambda) d\lambda \end{aligned} \quad (34)$$

where the cdf of $\gamma_{RD}^{(K)}$ is given by

$$\begin{aligned} F_{\gamma_{RD}^{(K)}}(x) &= \left[1 - e^{-\frac{x}{\beta_2}} \sum_{t=0}^{M_2-1} \frac{1}{t!} \left(\frac{x}{\beta_2}\right)^t\right]^{N_r} \\ &= \sum_{p=0}^{N_r} \sum_{q=0}^{p(M_2-1)} \binom{N_r}{p} \frac{(-1)^p \phi_{q,p,M_2}}{(\beta_2)^q} x^q e^{-\frac{px}{\beta_2}} \end{aligned} \quad (35)$$

and the pdf of $\gamma_{RD}^{(K)}$ can be obtained by differentiation of (35) as

$$\begin{aligned} f_{\gamma_{RD}^{(K)}}(x) &= \frac{d}{dx} \left\{F_{\gamma_{RD}^{(K)}}(x)\right\} \\ &= \sum_{p=0}^{N_r-1} \sum_{q=0}^{p(M_2-1)} \frac{(-1)^p \binom{N_r-1}{p}}{\Gamma(M_2)} \\ &\quad \times \frac{\phi_{q,p,M_2}}{(\beta_2)^{M_2+q}} x^{M_2+q-1} e^{-\frac{(p+1)x}{\beta_2}}. \end{aligned} \quad (36)$$

In (35) and (36), $M_2 = m_2 N_d$. The cdf of $\gamma_{SR}^{(I)}$ is given by

$$F_{\gamma_{SR}^{(I)}}(x) = \left[1 - e^{-\frac{x}{\beta_1}} \sum_{t=0}^{M_1-1} \frac{1}{t!} \left(\frac{x}{\beta_1} \right)^t \right]^{N_s} \\ = \sum_{a=0}^{N_s} \sum_{b=0}^{a(M_1-1)} \binom{N_s}{a} \frac{(-1)^a \phi_{b,a,M_1}}{(\beta_1)^b} x^b e^{-\frac{ax}{\beta_1}} \quad (37)$$

where $M_1 = m_2 N_d$. Next, by substituting (35)–(37) into (34), a single integral expression involving $\int_0^\infty \lambda^{M_2+q-b-1} (x+\lambda)^b \exp(-(p+1)\lambda/\beta_2) - (ax^2/\beta_1\lambda) d\lambda$ for $\gamma_{SRD}^{(I,K)}$ can be obtained. The foregoing integral can readily be evaluated in closed form by first using the binomial expansion of $(x+\lambda)^b$ and then using [20, eq. (3.471.9)]. Finally, the desired result (7a) can be obtained in closed form by substituting $\gamma_{SRD}^{(I,K)}$ and (33) into (32).

APPENDIX B

PROOF OF THE mgf OF THE e2e SNR FOR TAS_{subopt1}

In TAS_{subopt1}, the antenna indexes I and K are selected at S and R , respectively, by following (3). The e2e SNR of the TAS_{subopt1} is given by $\gamma_{eq}^{\text{subopt1}} = \gamma_{SD}^{\text{subopt1}} + \gamma_{SRD}^{\text{subopt1}}$, where $\gamma_{SRD}^{\text{subopt1}} = (\gamma_{SR}^{\text{subopt1}} \gamma_{RD}^{(K)} / \gamma_{SR}^{\text{subopt1}} + \gamma_{RD}^{(K)})$ is the SNR of the relayed path, and $\gamma_{SR}^{\text{subopt1}}$ is the SNR at R received by the I th transmit antenna at S . Because in TAS_{subopt1} the I th antenna at S is selected to maximize the SNR of $S \rightarrow D$ separately without considering the $S \rightarrow R$ channel, the pdf of $\gamma_{SR}^{\text{subopt1}}$ is given by $f_{\gamma_{SR}^{\text{subopt1}}}(x) = (x^{M_1-1} e^{-x/\beta_1} / \Gamma(M_1) (\beta_1)^{M_1})$. The cdf of $\gamma_{SD}^{\text{subopt1}}$ is the same as that of $\gamma_{SD}^{(I)}$ and is given in Appendix A. By substituting $F_{\gamma_{RD}^{(K)}}(x)$ and $f_{\gamma_{SR}^{\text{subopt1}}}(x)$ into the integral representation $F_{\gamma_{SRD}^{\text{subopt1}}}(x) = 1 - \int_0^\infty [1 - F_{\gamma_{RD}^{(K)}}((z+x)x/z)] f_{\gamma_{SR}^{\text{subopt1}}}(z+x) dz$ and evaluating the integral by using [20, eq. (3.471.9)], the $F_{\gamma_{SRD}^{\text{subopt1}}}(x)$ can be obtained as follows:

$$F_{\gamma_{SRD}^{\text{subopt1}}}(x) = 1 - \sum_{a=1}^{N_r} \sum_{b=0}^{a(M_2-1)} \sum_{c=0}^{b+M_1-1} \mathcal{A}_2 x^{b+M_1} e^{-\mu x} \mathcal{K}_{c-b+1}(\nu x) \quad (38)$$

where $\mu = (1/\beta_1) + (a/\beta_2)$, and $\nu = 2\sqrt{a/\beta_1\beta_2}$. Further, \mathcal{A}_2 is defined in (10b).

The mgfs of $\gamma_{SD}^{\text{subopt1}}$ and $\gamma_{SRD}^{\text{subopt1}}$ can be derived by substituting their cdfs into

$$\mathcal{M}_\Gamma(s) = \mathcal{E}_\Gamma\{e^{-s\gamma}\} = \int_0^\infty s F_\Gamma(\gamma) e^{-s\gamma} d\gamma \quad (39)$$

and solving the resulting integrals by using [20, eq. (6.621.3)], as given in (10a) and (11). The desired result can easily be obtained by multiplying (10a) and (11).

APPENDIX C

SINGLE POLYNOMIAL APPROXIMATION OF THE cdf OF THE e2e SNR FOR TAS_{subopt1}

The behavior of the cdf of $\gamma_{SRD}^{\text{subopt1}}$ for a large $\bar{\gamma}$ is equivalent to the behavior of $F_{\gamma_{SRD}^{\text{subopt1}}}(y)$ around $y = 0$ [29]. By substituting $\beta_1 = (k_1/m_1)\bar{\gamma}$, $\beta_2 = (k_2/m_2)\bar{\gamma}$, and $x = \bar{\gamma}y$, where $\bar{\gamma}$ is the transmit SNR, into (38), an alternative expression for $F_{\gamma_{SRD}^{\text{subopt1}}}(x)$ can be obtained as follows:

$$F_{\gamma_{SRD}^{\text{subopt1}}}(y) = 1 - \sum_{a=1}^{N_r} \sum_{b=0}^{a(M_2-1)} \sum_{c=0}^{b+M_1-1} \mathcal{A} y^{b+M_1} e^{-\mu' y} \mathcal{K}_{c-b+1}(\nu' y) \quad (40a)$$

where \mathcal{A} is defined as

$$\mathcal{A} = \frac{2(-1)^{a+1} \phi_{b,a,M_2} \binom{N_r}{a} \binom{b+M_1-1}{c} \left(\frac{m_1}{k_1} \right)^{\frac{2M_1+b-c-1}{2}}}{\Gamma(M_1) a^{\frac{b-c-1}{2}} \left(\frac{m_2}{k_2} \right)^{\frac{-(c+b+1)}{2}}} \quad (40b)$$

where $\mu' = (m_1/k_1) + (am_2/k_2)$, and $\nu' = 2\sqrt{am_1m_2/k_1k_2}$. Next, by expressing the exponential function and the Bessel function in terms of their Taylor series expansions around $y = 0$ [20, eqs. (1.211) and (8.446)], $F_{\gamma_{SRD}^{\text{subopt1}}}(x)$ can be approximated as a polynomial of the lowest powers of x as follows:

$$F_{\gamma_{SRD}^{\text{subopt1}}}(y) = 1 - \sum_{a=1}^{N_r} \sum_{b=0}^{a(M_2-1)} \sum_{c=0}^{b+M_1-1} \mathcal{A}' \sum_{l=0}^{\infty} \frac{(-\mu')^l}{l!} y^{M_1+2b+l-c-1} \quad (41a)$$

where \mathcal{A}' is given by

$$\mathcal{A}' = \frac{2^{c-b+1} (-1)^{a+1} \phi_{b,a,M_2} \Gamma(c-b+1) \binom{N_r}{a} \binom{b+M_1-1}{c}}{(\nu')^{c-b+1} \Gamma(M_1) a^{\frac{b-c-1}{2}}} \\ \times \left(\frac{m_1}{k_1} \right)^{\frac{2M_1+b-c-1}{2}} \left(\frac{m_2}{k_2} \right)^{\frac{c+b+1}{2}}. \quad (41b)$$

Now, by substituting $y = x/\bar{\gamma}$ into (41a) and finding the first nonzero derivative order of (41a) and discarding the higher-order terms, $F_{\gamma_{SRD}^{\text{subopt1}}}(x)$ can be approximated by a single polynomial term for $x \rightarrow 0^+$ as

$$F_{\gamma_{SRD}^{\text{subopt1}}}(x) = \begin{cases} \Lambda_1 \left(\frac{x}{\bar{\gamma}} \right)^{m_1 N_r} + o(x^{m_1 N_r + 1}), & m_1 < m_2 N_d \\ \Lambda_2 \left(\frac{x}{\bar{\gamma}} \right)^{m_2 N_r N_d} + o(x^{m_2 N_r N_d + 1}), & m_1 > m_2 N_d \\ \Lambda_3 \left(\frac{x}{\bar{\gamma}} \right)^{m_1 N_r} + o(x^{m_1 N_r + 1}), & m_1 = m_2 N_d. \end{cases} \quad (42)$$

$\Lambda_1 = (m_1/k_1)^{m_1 N_r} / (m_1 N_r)!$, $\Lambda_2 = (m_2/k_2)^{m_2 N_d N_r} / ((m_2 N_d)!)^{N_r}$, and $\Lambda_3 = \Lambda_1 + \Lambda_2$, where $k_1 = \bar{\gamma}_{SR}/\bar{\gamma}$, and

$k_2 = \bar{\gamma}_{RD}/\bar{\gamma}$. Thus, from (42), the diversity order of the relayed path ($S \rightarrow R \rightarrow D$) of $\text{TAS}_{\text{subopt}_1}$ is given by $G_{d,SRD}^{\text{TAS}_{\text{subopt}_1}} = N_r \min(m_1, m_2 N_d)$. The single polynomial approximation of the cdf of $\gamma_{SD}^{\text{subopt}_1}$ for $x \rightarrow 0^+$ is given by

$$F_{\gamma_{SD}^{\text{subopt}_1}}^{\infty}(x) = \frac{(m_0/k_0)^{m_0 N_d N_s}}{((m_0 N_d)!)^{N_s}} \left(\frac{x}{\bar{\gamma}}\right)^{m_0 N_d N_s} + o(x^{m_0 N_d N_s + 1}) \quad (43)$$

where $k_0 = \bar{\gamma}_{SD}/\bar{\gamma}$. The diversity order of the direct channel is given by $G_{d,SD}^{\text{TAS}_{\text{subopt}_1}} = m_0 N_d N_s$.

For the sake of notational simplicity, the single polynomial cdf approximations for $x \rightarrow 0^+$ of the relayed path and direct path SNRs are denoted by $F_{\gamma_{SRD}^{\infty}}(x) = \beta_{SRD}(x/\bar{\gamma})^{d_{SRD}} + o(x^{d_{SRD}+1})$ and $F_{\gamma_{SD}^{\infty}}(x) = \beta_{SD}(x/\bar{\gamma})^{d_{SD}} + o(x^{d_{SD}+1})$, respectively. The single polynomial approximations for the mgfs of γ_{SRD} and γ_{SD} can be derived by substituting $F_{\gamma_{SRD}^{\infty}}(x)$ and $F_{\gamma_{SD}^{\infty}}(x)$ into (39) as follows: $\mathcal{M}_{\gamma_{SRD}^{\infty}}(s) = \beta_{SRD}\Gamma(d_{SRD} + 1)/(\bar{\gamma}s)^{d_{SRD}} + o(s^{-(d_{SRD}+1)})$, and $\mathcal{M}_{\gamma_{SD}^{\infty}}(s) = \beta_{SD}\Gamma(d_{SD} + 1)/(\bar{\gamma}s)^{d_{SD}} + o(s^{-(d_{SD}+1)})$. Next, a single polynomial approximation of the cdf of the e2e SNR ($\gamma_{\text{eq}} = \gamma_{SD} + \gamma_{SRD}$) for $x \rightarrow 0^+$ can be derived by using $\mathcal{L}^{-1}(\mathcal{M}_{\gamma_{SD}^{\infty}}(s)\mathcal{M}_{\gamma_{SRD}^{\infty}}(s)/s)$, where $\mathcal{L}^{-1}(\cdot)$ denotes the inverse Laplace transform, as follows:

$$F_{\gamma_{\text{eq}}^{\infty}}(x) = \frac{\beta_{SD}\beta_{SRD}\Gamma(d_{SD} + 1)\Gamma(d_{SRD} + 1)}{\Gamma(d_{SD} + d_{SRD} + 1)} \times \left(\frac{x}{\bar{\gamma}}\right)^{d_{SD} + d_{SRD}} + o(x^{d_{SD} + d_{SRD} + 1}). \quad (44)$$

Now, by substituting corresponding values of β_{SD} , β_{SRD} , d_{SD} , and d_{SRD} given in (42) and (43) into (44), the desired result can be obtained as in (19a).

APPENDIX D

PROOF OF THE mgf OF THE e2e SNR FOR $\text{TAS}_{\text{subopt}_2}$

In $\text{TAS-AF}_{\text{subopt}_2}$, the antenna indexes I and K are selected at S and R , respectively, according to (4). The corresponding e2e SNR is given by $\gamma_{\text{eq}}^{\text{subopt}_2} = \gamma_{SD}^{\text{subopt}_2} + \gamma_{SRD}^{\text{subopt}_2}$, where $\gamma_{SRD}^{\text{subopt}_2} = (\gamma_{SR}^{(I)}\gamma_{RD}^{(K)}/\gamma_{SR}^{(K)} + \gamma_{RD}^{(K)})$ is the SNR of the relayed path, and $\gamma_{SD}^{\text{subopt}_2}$ is the SNR received at D by the I th antenna at S . In $\text{TAS}_{\text{subopt}_2}$, the I th antenna at S is selected to maximize the SNR of $S \rightarrow R$ separately, without considering the $S \rightarrow D$ channel. Thus, the pdf of $\gamma_{SD}^{\text{subopt}_2}$ is given by $f_{\gamma_{SD}^{\text{subopt}_2}}(x) = (x^{M_0-1}e^{-x/\beta_2}/\Gamma(M_0)(\beta_2)^{M_0})$, and the corresponding mgf is given by $\mathcal{M}_{\gamma_{SD}^{\text{subopt}_2}}(s) = 1/(1 + \beta_0 s)^{M_0}$. The cdf of $\gamma_{SRD}^{\text{subopt}_2}$ can be derived by substituting $f_{\gamma_{SR}^{(I)}}(x)$ and $F_{\gamma_{RD}^{(K)}}(x)$, as given in Appendix A, into $F_{\gamma_{SRD}^{\text{subopt}_2}}(x) = 1 - \int_0^{\infty} [1 - F_{\gamma_{RD}^{(K)}}((z+x)x/z)]f_{\gamma_{SR}^{(I)}}(z+x)dz$ and evaluating the integral by using [20, eq. (6.621.3)] as

$$F_{\gamma_{SRD}^{\text{subopt}_2}}(x) = 1 - \sum_{p,q,a,b,c} \mathcal{A}_3 x^{M_1+b+q} e^{-\delta x} \mathcal{K}_{c-q+1}(\epsilon x). \quad (45)$$

$\sum_{p,q,a,b,c}$ and \mathcal{A}_3 are defined in (12b) and (12a), where $\delta = (a + 1/\beta_1) + (p/\beta_2)$, and $\epsilon = 2\sqrt{p(a+1)/\beta_1\beta_2}$. The corresponding mgf of e2e SNR can readily be obtained by following similar steps to those used for the mgfs in Appendix B.

APPENDIX E

SINGLE POLYNOMIAL APPROXIMATION OF THE cdf OF THE e2e SNR FOR $\text{TAS}_{\text{subopt}_2}$

The cdf of $\gamma_{SRD}^{\text{subopt}_2}$ (45) can be approximated by a single polynomial term for $x \rightarrow 0^+$ by following similar steps to those in Appendix C as

$$F_{\gamma_{SRD}^{\text{subopt}_2}}^{\infty}(x) = \begin{cases} \Pi_1 \left(\frac{x}{\bar{\gamma}}\right)^{m_1 N_s N_r} + o(x^{m_1 N_s N_r + 1}), & m_1 N_s < m_2 N_d \\ \Pi_2 \left(\frac{x}{\bar{\gamma}}\right)^{m_2 N_r N_d} + o(x^{m_2 N_r N_d + 1}), & m_1 N_s > m_2 N_d \\ \Pi_3 \left(\frac{x}{\bar{\gamma}}\right)^{m_1 N_s N_r} + o(x^{m_1 N_s N_r + 1}), & m_1 N_s = m_2 N_d \end{cases} \quad (46)$$

where $\Pi_1 = (m_1/k_1)^{m_1 N_s N_r}/((m_1 N_r)!)^{N_s}$, $\Pi_2 = (m_2/k_2)^{m_2 N_r N_d}/((m_2 N_d)!)^{N_r}$, and $\Pi_3 = \Pi_1 + \Pi_2$. Thus, from (46), the diversity order of the relayed path of $\text{TAS}_{\text{subopt}_2}$ is given by $G_{d,SRD}^{\text{TAS}_{\text{subopt}_2}} = N_r \min(m_1 N_s, m_2 N_d)$. The cdf of $\gamma_{SD}^{\text{subopt}_2}$ can be approximated by a single polynomial term for $x \rightarrow 0^+$ as

$$F_{\gamma_{SD}^{\text{subopt}_2}}^{\infty}(x) = \frac{(m_0/k_0)^{m_0 N_d}}{(m_0 N_d)!} \left(\frac{x}{\bar{\gamma}}\right)^{m_0 N_d} + o(x^{m_0 N_d + 1}). \quad (47)$$

The diversity order of the direct path is given by $G_{d,SD}^{\text{TAS}_{\text{subopt}_1}} = m_0 N_d$. Now, by following steps similar to those in Appendix C, the desired results in (20a) can be derived.

APPENDIX F

SINGLE POLYNOMIAL APPROXIMATION OF THE cdf OF THE e2e SNR FOR TAS_{opt}

At high SNRs, the TAS corresponding to the relayed path can be approximated as $I = \arg \max_{1 \leq i \leq N_s} (\gamma_{SR}^{(i)})$ and $K = \arg \max_{1 \leq k \leq N_r} (\gamma_{RD}^{(k)})$. Thus, the cdf of the relayed path SNR ($\gamma_{SRD}^{\text{opt}}$) for $x \rightarrow 0^+$ can be approximated by (46). Further, the cdf of the direct path SNR (γ_{SD}^{opt}) for $x \rightarrow 0^+$ can be approximated by (43). Next, by following similar steps to those in Appendix C, the cdf of the e2e SNR ($\gamma_{\text{eq}}^{\text{opt}}$) can be approximated by a single polynomial term for $x \rightarrow 0^+$, as given in (21a).

APPENDIX G

PROOF OF THE cdf OF THE e2e SNR $\tilde{\gamma}_{\text{eq}}^{\text{opt}}$ WHEN THE TAS IS BASED ON THE OUTDATED CSI

Let $\tilde{\gamma}_{SR}^{(i)}$ denote the delayed version of $\gamma_{SR}^{(i)}$ by time τ_1 . The average fading power is assumed to remain constant over the

time delay τ_1 . By following the outdated CSI approach in [32], the joint pdf of $\tilde{\gamma}_{SR}^{(i)}$ and $\gamma_{SR}^{(i)}$ can be written as follows:

$$f_{\tilde{\gamma}_{SR}^{(i)}, \gamma_{SR}^{(i)}}(x, y) = \frac{m_1^{m_1 N_r + 1} (xy)^{\frac{m_1 N_r - 1}{2}}}{(m_1 N_r - 1)! \rho_1^{\frac{m_1 N_r - 1}{2}} (1 - \rho_1) (\tilde{\gamma}_{SR})^{m_1 N_r + 1}} \times e^{-\frac{x+y}{(1-\rho_1)\tilde{\gamma}_{SR}} \mathbb{I}_{m_1 N_r - 1}} \left(\frac{2m_1 N_r \sqrt{xy\rho_1}}{(1-\rho_1)\tilde{\gamma}_{SR}} \right) \quad (48)$$

where ρ_1 is the normalized correlation coefficient between $\tilde{\gamma}_{SR}^{(i)}$ and $\gamma_{SR}^{(i)}$. The feedback delay τ_1 can be related to ρ_1 by following Clarke's fading model, as $\rho_1 = \mathcal{J}_0(2\pi B_{f_1} \tau_1)$, where B_{f_1} is the Doppler fading frequency. In fact, (48) is the joint pdf of two correlated Gamma distributed random variables.

The cdf of $\tilde{\gamma}_{SR}^{\text{opt}}$ can be derived by using $F_{\tilde{\gamma}_{SR}^{\text{opt}}}(x) = 1 - \int_0^\infty [1 - F_{\tilde{\gamma}_{SR}^{(l)}}((z+x)x/z)] f_{\tilde{\gamma}_{RD}^{(K)}}(z+x) dz$. Now, one needs to obtain the cdf of $\tilde{\gamma}_{SR}^{(l)}$ and the pdf of $\tilde{\gamma}_{RD}^{(K)}$. To this end, we start deriving the cdf of $\tilde{\gamma}_{SR}^{(l)}$. In fact, $\tilde{\gamma}_{SR}^{(l)}$ is the induced order statistic of the original order statistic $\gamma_{SR}^{(l)}$ [33]. The pdf of $\tilde{\gamma}_{SR}^{(l)}$ can be obtained by using [32], [33]

$$f_{\tilde{\gamma}_{SR}^{(l)}}(x) = \int_0^\infty f_{\tilde{\gamma}_{SR}^{(l)}|\gamma_{SR}^{(l)}}(x|y) f_{\gamma_{SR}^{(l)}}(y) dy \quad (49)$$

where $f_{\tilde{\gamma}_{SR}^{(l)}|\gamma_{SR}^{(l)}}(x|y) = f_{\tilde{\gamma}_{SR}^{(i)}, \gamma_{SR}^{(i)}}(x, y) / f_{\gamma_{SR}^{(i)}}(y)$ is the pdf of $\tilde{\gamma}_{SR}^{(l)}$ conditioned on $\gamma_{SR}^{(l)}$. The pdf of $\gamma_{SR}^{(l)}$ is given by $f_{\gamma_{SR}^{(l)}}(y) = N_r [F_{\gamma_{SR}^{(i)}}(y)]^{N_r - 1} f_{\gamma_{SR}^{(i)}}(y)$. By substituting (48) into (49) and solving the resulting integral by using [34, eq. (4.16.20)], the pdf of $\tilde{\gamma}_{SR}^{(l)}$ can be obtained as follows:

$$f_{\tilde{\gamma}_{SR}^{(l)}}(x) = \sum_{a=0}^{N_s - 1} \sum_{b=0}^{a(M_1 - 1)} \frac{N_s (-1)^a \binom{N_s - 1}{a} \phi_{b, a, M_1} \Gamma(M_1 + b)}{\Gamma^2(M_1) \rho_1^{\frac{M_1}{2}} \beta_1^{\frac{M_1}{2}}} \times \frac{(1 - \rho_1)^\xi}{(1 + a(1 - \rho_1))^\xi} x^{\frac{M_1 - 2}{2}} e^{-\Xi x} \mathbb{M}_{-\xi, \vartheta}(\theta x) \quad (50)$$

where $\xi = (M_1 + 2b/2)$, $\vartheta = (M_1 - 1/2)$, $\Xi = (2 + 2a(1 - \rho) - \rho) / (2\beta_1(1 - \rho)(1 + a(1 - \rho)))$, and $\theta = \rho / \beta_1(1 - \rho)(1 + a(1 - \rho))$. First, by using the confluent hypergeometric function ${}_1\mathcal{F}_1(\cdot; \cdot; \cdot)$ representation of Whittaker-M function [20, eq. (9.220.2)] and then by expressing ${}_1\mathcal{F}_1(\cdot; \cdot; \cdot)$ as a finite series expansion [35], a mathematically tractable form for (50) can be obtained as follows:

$$f_{\tilde{\gamma}_{SR}^{(l)}}(x) = \sum_{a=0}^{N_s - 1} \sum_{b=0}^{a(M_1 - 1)} \sum_{k=0}^b \frac{N_s (-1)^a \binom{N_s - 1}{a} \binom{b}{k} \phi_{b, a, M_1}}{\Gamma(M_1) \Gamma(M_1 + k) \beta_1^{M_1 + k}} \times \frac{\Gamma(M_1 + b) \rho_1^k (1 - \rho_1)^{b-k}}{(1 + a(1 - \rho))^{M_1 + b + k}} x^{M_1 + k - 1} e^{-\Phi x} \quad (51)$$

where $\Phi = (a + 1) / \beta_1(1 + a(1 - \rho_1))$. Now, the cdf of $\tilde{\gamma}_{SR}^{(l)}$ can readily be derived as

$$F_{\tilde{\gamma}_{SR}^{(l)}}(x) = 1 - \sum_{a=0}^{N_s - 1} \sum_{b=0}^{a(M_1 - 1)} \sum_{k=0}^b \sum_{l=0}^{M_1 + k - 1} \frac{N_s (-1)^a \binom{N_s - 1}{a} \binom{b}{k}}{\Gamma(M_1) \beta_1^l (l!)} \times \frac{\phi_{b, a, M_1} \Gamma(M_1 + b) \rho_1^k (1 - \rho_1)^{b-k}}{(a + 1)^{M_1 + k - l} (1 + a(1 - \rho_1))^{b+l}} x^l e^{-\Phi x}. \quad (52)$$

By using similar steps to those of the derivation of $f_{\tilde{\gamma}_{SR}^{(l)}}(x)$, the pdf of $\tilde{\gamma}_{RD}^{(K)}$, i.e., $f_{\tilde{\gamma}_{RD}^{(K)}}(x)$, can be derived as well. Now, the cdf of e2e SNR, when the direct path is ignored, can be derived by using $F_{\gamma_{\text{eq}}^{\text{opt}}}(x) = 1 - \int_0^\infty [1 - F_{\tilde{\gamma}_{SR}^{(l)}}((z+x)x/z)] f_{\tilde{\gamma}_{RD}^{(K)}}(z+x) dz$, as given in (28a).

REFERENCES

- [1] Y. Yang, H. Hu, J. Xu, and G. Mao, "Relay technologies for WiMAX and LTE-advanced mobile systems," *IEEE Commun. Mag.*, vol. 47, no. 10, pp. 100–105, Oct. 2009.
- [2] K. Loa, C.-C. Wu, S.-T. Sheu, Y. Yuan, M. Chion, D. Huo, and L. Xu, "IMT-advanced relay standards," *IEEE Commun. Mag.*, vol. 48, no. 8, pp. 40–48, Aug. 2010.
- [3] Y. Fan and J. Thompson, "MIMO configurations for relay channels: Theory and practice," *IEEE Trans. Wireless Commun.*, vol. 6, no. 5, pp. 1774–1786, May 2007.
- [4] M. Yuksel and E. Erkip, "Multiple-antenna cooperative wireless systems: A diversity-multiplexing tradeoff perspective," *IEEE Trans. Inf. Theory*, vol. 53, no. 10, pp. 3371–3393, Oct. 2007.
- [5] S. Peters and R. W. Heath, "Nonregenerative MIMO relaying with optimal transmit antenna selection," *IEEE Signal Process. Lett.*, vol. 15, pp. 421–424, 2008.
- [6] L. Cao, X. Zhang, Y. Wang, and D. Yang, "Transmit antenna selection strategy in amplify-and-forward MIMO relaying," in *Proc. IEEE Wireless Commun. Netw. Conf.*, Budapest, Hungary, Apr. 2009, pp. 1–4.
- [7] I.-H. Lee and D. Kim, "Outage probability of multi-hop MIMO relaying with transmit antenna selection and ideal relay gain over Rayleigh fading channels," *IEEE Trans. Commun.*, vol. 57, no. 2, pp. 357–360, Feb. 2009.
- [8] S. Chen, W. Wang, X. Zhang, and D. Zhao, "Performance of amplify-and-forward MIMO relay channels with transmit antenna selection and maximal-ratio combining," in *Proc. IEEE WCNC*, Apr. 2009, pp. 1–6.
- [9] J.-B. Kim and D. Kim, "BER analysis of dual-hop amplify-and-forward MIMO relaying with best antenna selection in Rayleigh fading channels," *IEICE Trans. Commun.*, vol. E91.B, no. 8, pp. 2772–2775, Aug. 2008.
- [10] H. A. Suraweera, G. K. Karagiannidis, Y. Li, H. K. Garg, A. Nallanathan, and B. Vucetic, "Amplify-and-forward relay transmission with end-to-end antenna selection," in *Proc. IEEE WCNC*, Apr. 2010, pp. 1–6.
- [11] S. Thoen, L. Van der Perre, B. Gyselinckx, and M. Engels, "Performance analysis of combined transmit-SC/receive-MRC," *IEEE Trans. Commun.*, vol. 49, no. 1, pp. 5–8, Jan. 2001.
- [12] Z. Chen, Z. Chi, Y. Li, and B. Vucetic, "Error performance of maximal-ratio combining with transmit antenna selection in flat Nakagami- m fading channels," *IEEE Trans. Wireless Commun.*, vol. 8, no. 1, pp. 424–431, Jan. 2009.
- [13] G. Amarasuriya, C. Tellambura, and M. Ardakani, "Transmit antenna selection strategies for cooperative MIMO AF relay networks," in *Proc. IEEE Global Commun. Conf.*, Miami, FL, Dec. 2010, pp. 1–5.
- [14] C. Feng, L. Cao, X. Zhang, and D. Yang, "Diversity order analysis of a suboptimal transmit antenna selection strategy for non-regenerative MIMO relay channel," in *Proc. IEEE 20th Int. Symp. Pers., Indoor, Mobile Radio Commun.*, Sep. 2009, pp. 978–982.
- [15] A. Muller and J. Speidel, "Outage-optimal transmit antenna selection for cooperative decode-and-forward systems," in *Proc. IEEE 69th VTC—Spring*, Apr. 2009, pp. 1–5.
- [16] T. Duong, H.-J. Zepemick, T. Tsiftsis, and Q. B. V. Nguyen, "Performance analysis of amplify-and-forward MIMO relay networks with transmit antenna selection over Nakagami- m channels," in *Proc. IEEE PIMRC*, Sep. 2010, pp. 368–372.
- [17] L. Cao, L. Chen, X. Zhang, and D. Yang, "Performance analysis of two-hop amplify-and-forward MIMO relaying with transmit antenna selection," in *Proc. IEEE PIMRC*, Sep. 2010, pp. 373–378.

- [18] L. Cao, L. Chen, X. Zhang, and D. Yang, "Asymptotic performance of two-hop amplify-and-forward MIMO relaying with transmit antenna selection," in *Proc. IEEE GLOBECOM*, Dec. 2010, pp. 1–6.
- [19] A. Yilmaz and O. Kucur, "Error performance of joint transmit and receive antenna selection in two hop amplify-and-forward relay system over Nakagami- m fading channels," in *Proc. IEEE PIMRC*, Sep. 2010, pp. 2198–2203.
- [20] I. Gradshteyn and I. Ryzhik, *Table of Integrals, Series, and Products*, 7th ed. New York: Academic, 2007.
- [21] M. Abramowitz and I. Stegun, *Handbook of Mathematical Functions*. New York: Dover, 1970.
- [22] J. N. Laneman, D. N. C. Tse, and G. W. Wornell, "Cooperative diversity in wireless networks: Efficient protocols and outage behavior," *IEEE Trans. Inf. Theory*, vol. 50, no. 12, pp. 3062–3080, Dec. 2004.
- [23] M. O. Hasna and M. S. Alouini, "End-to-end performance of transmission systems with relays over Rayleigh-fading channels," *IEEE Trans. Wireless Commun.*, vol. 2, no. 6, pp. 1126–1131, Nov. 2003.
- [24] R. H. Y. Louie, Y. Li, H. A. Suraweera, and B. Vucetic, "Performance analysis of beamforming in two hop amplify and forward relay networks with antenna correlation," *IEEE Trans. Wireless Commun.*, vol. 8, no. 6, pp. 3132–3141, Jun. 2009.
- [25] A. Annamalai and C. Tellambura, "Error rates for Nakagami- m fading multichannel reception of binary and M-ary signals," *IEEE Trans. Commun.*, vol. 49, no. 1, pp. 58–68, Jan. 2001.
- [26] J. Abate and P. P. Valko, "Multi-precision Laplace transform inversion," *Int. J. Numer. Methods Eng.*, vol. 60, no. 5, pp. 979–993, Jun. 2004.
- [27] R. C. Palat, A. Annamalai, and J. H. Reed, "An efficient method for evaluating information outage probability and ergodic capacity of OSTBC system," *IEEE Commun. Lett.*, vol. 12, no. 3, pp. 191–193, Mar. 2008.
- [28] A. Annamalai, C. Tellambura, and V. K. Bhargava, "Efficient computation of MRC diversity performance in Nakagami fading channel with arbitrary parameters," *Electron. Lett.*, vol. 34, no. 12, pp. 1189–1190, Jun. 1998.
- [29] Z. Wang and G. B. Giannakis, "A simple and general parameterization quantifying performance in fading channels," *IEEE Trans. Commun.*, vol. 51, no. 8, pp. 1389–1398, Aug. 2003.
- [30] S. Zhou and G. Giannakis, "Adaptive modulation for multiantenna transmissions with channel mean feedback," *IEEE Trans. Wireless Commun.*, vol. 3, no. 5, pp. 1626–1636, Sep. 2004.
- [31] G. Amarasuriya, C. Tellambura, and M. Ardashani, "Feedback delay effect on dual-hop MIMO AF relaying with antenna selection," in *Proc. IEEE GLOBECOM*, Miami, FL, Dec. 2010, pp. 1–5.
- [32] J. Ritcey and M. Azizoglu, "Impact of switching constraints on selection diversity performance," in *Conf. Rec. 32nd Asilomar Conf. Signals, Syst., Comput.*, Nov. 1998, pp. 795–799.
- [33] H. A. David, *Order Statistics*, 2nd ed. New York: Wiley, 1981.
- [34] A. Erdelyi, W. Magnus, and F. G. Tricomi, *Tables of Integral Transforms, Vol-1*. New York: McGraw-Hill, 1954.
- [35] [Online]. Available: <http://functions.wolfram.com/07.20.03.0025.01>



Chinthu Tellambura (SM'02–F'11) received the B.Sc. degree (with first-class honors) from the University of Moratuwa, Moratuwa, Sri Lanka, in 1986, the M.Sc. degree in electronics from the University of London, London, U.K., in 1988, and the Ph.D. degree in electrical engineering from the University of Victoria, Victoria, BC, Canada, in 1993.

He was a Postdoctoral Research Fellow with the University of Victoria from 1993 to 1994 and the University of Bradford, Bradford, U.K., from 1995 to 1996. He was with Monash University, Melbourne, Australia, from 1997 to 2002. He is currently a Professor with the Department of Electrical and Computer Engineering, University of Alberta, Edmonton, AB, Canada. His research interests include diversity and fading countermeasures, multiple-input–multiple-output systems and space–time coding, and orthogonal frequency division multiplexing.

Prof. Tellambura is an Associate Editor for the IEEE TRANSACTIONS ON COMMUNICATIONS and the Area Editor for wireless communications systems and theory of the IEEE TRANSACTIONS ON WIRELESS COMMUNICATIONS. He was the Chair of the Communication Theory Symposium at the 2005 IEEE Global Telecommunications Conference, held in St. Louis, MO.



Masoud Ardashani (M'04–SM'09) received the B.Sc. degree in electrical engineering from Isfahan University of Technology, Isfahan, Iran, in 1994, the M.Sc. degree in electrical engineering from Tehran University, Tehran, Iran, in 1997, and the Ph.D. degree in electrical engineering from the University of Toronto, Toronto, ON, Canada, in 2004.

He was a Postdoctoral Fellow with the University of Toronto from 2004 to 2005. He is currently an Associate Professor of electrical and computer engineering and an Alberta Ingenuity New Faculty with the University of Alberta, Edmonton, AB, Canada, where he holds an Informatics Circle of Research Excellence Junior Research Chair in wireless communications. His research interests are in the general area of digital communications, codes defined on graphs, and iterative decoding techniques.

Dr. Ardashani serves as an Associate Editor for the IEEE TRANSACTIONS ON WIRELESS COMMUNICATIONS and the IEEE COMMUNICATION LETTERS.



Gayan Amarasuriya (S'09) received the B.Sc. degree in electronic and telecommunication engineering (with first-class honors) from the University of Moratuwa, Moratuwa, Sri Lanka, in 2006. He is currently working toward the Ph.D. degree with the Electrical and Computer Engineering Department, University of Alberta, Edmonton, AB, Canada.

His research interests include the design and analysis of new transmission strategies for cooperative multiple-input–multiple-output relay networks and physical layer network coding.